

# Modeling information spread across networks with communities using a multitype branching process framework

Alina Dubovskaya\*

*Department of Psychology, University of Limerick and  
Mathematics Application Consortium for Science and Industry (MACSI), University of Limerick*

Caroline B. Pena

*Mathematics Application Consortium for Science and Industry (MACSI), University of Limerick*

David J.P. O’Sullivan

*Mathematics Application Consortium for Science and Industry (MACSI), University of Limerick*

(Dated: August 9, 2024)

The dynamics of information diffusion in complex networks is widely studied in an attempt to understand how individuals communicate and how information travels and reaches individuals through interactions. However, complex networks often present community structure, and tools to analyse information diffusion on networks with communities are needed. In this paper, we develop theoretical tools using multi-type branching processes to model and analyse simple contagion information spread on a broad class of networks with community structure. We show how, by using limited information about the network — the degree distribution within and between communities — we can calculate standard statistical characteristics of the dynamics of information diffusion, such as the extinction probability, hazard function, and cascade size distribution. These properties can be estimated not only for the entire network but also for each community separately. Furthermore, we estimate the probability of information spreading from one community to another where it is not currently spreading. We demonstrate the accuracy of our framework by applying it to two specific examples: the Stochastic Block Model and a log-normal network with community structure. We show how the initial seeding location affects the observed cascade size distribution on a heavy-tailed network and that our framework accurately captures this effect.

Keywords: spreading processes, branching processes, community structure, complex networks, cascades

## I. INTRODUCTION AND BACKGROUND

Understanding the dynamics of information spread across complex networks is crucial in today’s interconnected world [1]. Platforms such as Facebook and X (formerly Twitter) which connect millions of users and facilitate information spreading among them, have a profound impact on human societies. Social media shapes public opinion on personal as well as societal issues, including public health [2–5], politics [1, 6], and business [7]. It is, therefore, crucial to understand how information propagates among agents connected via complex networks and what factors accelerate or slow down the spread. Consequently, many efforts have been devoted to developing mathematical tools to analyse propagation on networks [8–10]. Information diffusion shares many characteristics with epidemic processes. However, in the study of information diffusion, we almost always deal with the process unfolding on a complex network of connections, where the structure of the network becomes crucial in determining the dynamics. These networks can be complex, but there are ways

to measure and summarise them, with many characteristics being well-known.

Community structure is one of the most discussed structural properties of social networks. Previous studies have highlighted the importance of community structure roles in explaining the spread of social contagions via reinforcement and homophily using both empirical and statistical analyses [11, 12]. Some have used communities as a feature to predict cascade size using machine learning and statistical methods [13, 14]. Community structure in real-world networks has been shown to have a substantial impact on percolation and epidemic spreading processes, where the community structure can both benefit and slow down the diffusion processes [15]. Additionally, mathematical models for spreading processes have also been developed, where probability-generating functions (PGFs) are used to capture the network and community structure, and then standard ordinary differential equations compartmental models are applied to model the diffusion processes [16]. However, the literature is scarce when it comes to theoretical studies of information spread on a network with community structure using branching processes [17–19]. One notable exception is Brummitt et al.’s [20] work on the modelling of interconnected electricity grids, which

---

\* Correspondence email address: Alina.Dubovskaya@ul.ie

showed the impact of sparsely connected electricity networks on the occurrence of blackouts of various sizes.

The branching processes framework allows us to estimate the distributional properties of the process. Instead of focusing on the average behaviour of cascades, which has been the main focus of many previous works, in this paper, we are interested in estimating distributions of the typical statistical characteristics of the cascade dynamics, e.g., cascade size distribution and extinction time distribution. Branching process approximation has previously proven effective in studying information diffusion across local tree-like networks [21], as well as on both homogeneous clique type networks and networks with heterogeneous degree and clustering [22, 23]. These works laid down a theoretical formalism that we can extend to networks with community structure. The introduction of community structure brings extra complexity to the analysis of information cascades. Information diffusion may halt within a community but be reintroduced later from another community, which, for example, will affect the calculation of the probability that information stops spreading (extinction probability) in a community. This complexity requires the development of new mathematical methods to describe information diffusion across communities.

In this paper, we develop theoretical tools to model and analyse information spread on a broad class of networks with community structure for a simple contagion mechanism that follows the Independent Cascade Model (ICM) [24, 25]. In the ICM model, each exposure of a susceptible individual to a disease (or piece of information) by an infected friend (or followed person) results in an independent chance of disease transmission (information adoption). We use a multi-type branching process approximation [26] and probability-generating functions to describe the spread under the ICM. We derive analytical expressions for fundamental characteristics of information spread, such as the probability of extinction, hazard function and cascade sizes distribution. Furthermore, we derive specific features associated with cross-community diffusion, such as the introduction probability — the probability of information (re)introduction to a community where it is not currently spreading. We demonstrate the effectiveness of our analysis initially on the Stochastic Block Model and then extend it to a general locally tree-like network with communities with known degree distributions.

The rest of this paper is structured as follows. We begin by describing the model in Sec. II, where we outline the assumptions we make about the underlying network and what is required for our method to be applicable. In Sec. III, we explain our approach using the Stochastic Block Model, a simple network with community structure. We demonstrate how we can simultaneously track cascade dynamics in multiple communities using multivariate probability generation functions. We derive

extinction probabilities, hazards, and cascade size distributions separately for each community as well as for the entire network. In Sec. IV, we extend the analysis from the previous section to a broad class of local-tree networks with communities. We then consider a typical example of a heavy-tailed network with communities and discuss how the community structure affects the cascade size distribution. Finally, Sec. V provides our concluding remarks and outlines areas for future research.

## II. CONCEPTUAL MODEL DESCRIPTION FOR INFORMATION SPREAD ON NETWORKS WITH COMMUNITIES

In this paper, we study information diffusion following the Independent Cascade Model on community-based networks. The schematic of the process along with the type of network we study is illustrated in Fig. 1a). The *Independent Cascade Model (ICM)* defines nodes of a network as being in one of three states: inactive, active, and removed. Active nodes independently attempt to activate their inactive neighbors with probability  $\rho$ , transitioning to the removed state afterward. Once the node is in the removed state, it cannot be reactivated. The process begins with a randomly selected active node from community 1 and terminates when no new active nodes are generated. We consider information diffusion that can be modelled as a *sub-critical branching process*, which is certain to terminate and only spread to a fraction of the possible nodes in a network. Such processes are interesting as many of the social processes that we wish to capture are sub-critical, where, even the largest diffusions only reach a small fraction of the potential audience, e.g., even the largest Twitter diffusion only reaches a small fraction of users [21].

We consider an undirected network with two communities; however, our approach can be easily applied to an arbitrary number of communities. The networks with communities should satisfy the following conditions: (a) they can be well described via a configuration model; (b) they have locally tree-like structure (either no or a limited amount number of triangles, clustering, in the network).

We describe the networks by the degree distributions within each community and between communities. Let  $D_1^{(1)}$  be the random variable for the number of connections a randomly chosen node from community 1 has to other nodes within community 1, i.e., let  $P(D_1^{(1)} = k)$  be the probability that a random node from community 1 has  $k$  connections to nodes in community 1. This random variable will follow the *in-community degree distribution* for community 1. Now let  $D_2^{(1)}$  be the random

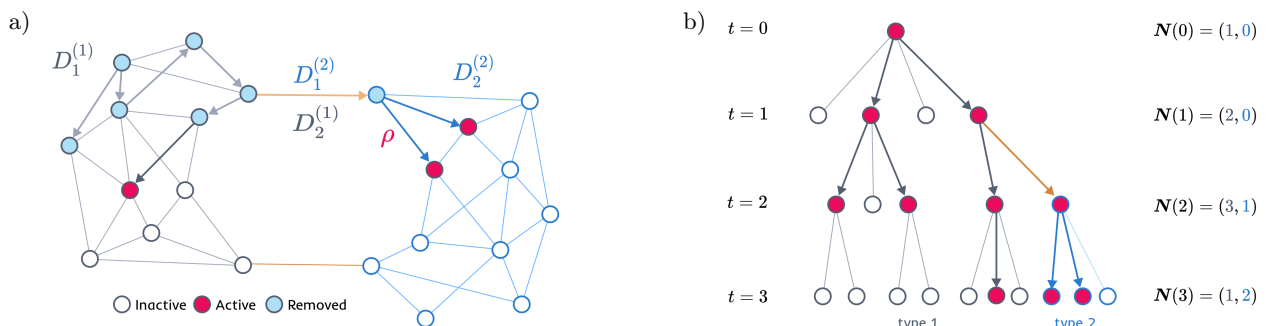


Figure 1: a) Schematic illustration of the Independent Cascade Model (ICM) on a community-based network. The network consists of two communities each described by its internal degree distributions and distribution of edges between communities. Here  $D_1^{(1)}$  and  $D_2^{(2)}$  are random variables for the nodes degree inside community 1 and 2 respectively;  $D_2^{(1)}$  and  $D_1^{(2)}$  are random variables for a nodes degree between-community (they are the same in the case of undirected networks considered here). At each time step, active nodes attempt to activate neighbours with probability  $\rho$ , then become inactive (or “removed”). The information spreads in the first community initially and later propagates to the second community. b) Schematic of the multi-type branching process approximating ICM on a community-based network. We track two types of offspring: “type 1” for active nodes in community 1, and “type 2” for active nodes in community 2. Here  $\mathbf{N}(t) = (N_1(t), N_2(t))$  tracks the number of active nodes of type 1 ( $N_1(t)$ ) and type 2 ( $N_2(t)$ ) at each time step.

variable for the number of connections a randomly chosen node from community 1 has to nodes in community 2, which follows the *between-community degree distribution*. In this notation, the superscript indicates the community of the node, while the subscript denotes the community of the nodes to which the end of the edges terminates. Such notation will be used consistently throughout the paper. Likewise, the in-community and between-community degree of a node for community 2 will be denoted by the random variables  $D_2^{(2)}$  and  $D_1^{(2)}$ , respectively. The connection process follows a configuration model [27], where each node has a random number of edges drawn independently from the nodes in- and between-community degree distributions. For example, a node in community 1 has the following probability of having  $k$  in-community edges and  $j$  between-community edges  $P[D_1^{(1)} = k] \times P[D_2^{(1)} = j]$ , as these distributions are treated as being independent of each other. The end of these  $k$  and  $j$  edges are randomly connected to  $k$  other nodes inside community 1 and  $j$  nodes in community 2.

Our goal is to calculate typical statistical characteristics of information diffusion, such as total cascade size distribution (also referred to as the total outbreak size or total progeny distribution) and extinction probability. Additionally, we aim to extract quantities that are particularly interesting for information diffusion on community-based networks, such as the probability of a contagion “escaping” its seed community or the probability of reintroduction of a contagion into a community where it has previously stopped spreading.

To calculate these quantities, we will describe the information diffusion process through a multi-type branching process. A *multi-type branching process (MTBP)* is a discrete Markov process that tracks the active nodes from each community at each time step as random variables [23, 26, 28]. We will refer to the active nodes in community 1 as “*type 1*” active nodes, and the active nodes in community 2 will be called “*type 2*” active nodes. At each time step, also referred to as a *generation* of the process, each type of node independently produces a random number of active *children* node. These active children are referred to as the active parents offspring in the Branching Processes literature [26]. The offspring follow a specific probability distribution, known as the *offspring distribution*. These offspring then continue the process, generating new descendants in subsequent generations, as illustrated in Fig. 1b). The primary components in this formulation are the offspring distributions, one specified for each type of node that we track. These distributions are then used to determine the number of active nodes of each type in a given generation (time step). The goal, generally in a Branching Processes, is to calculate the probability distribution of the total number of offspring of each type produced in each generation, as this fully determines the dynamics of the branching process [26]. Once this distribution is obtained, we can proceed with calculating key characteristics, such as cascade size and extinction probabilities, etc.

In the following sections, we develop a framework based on multi-type branching processes to describe

cascade dynamics in each community separately as well as in the entire network. We first develop our method for a simple Stochastic Block Model (SBM) [29]. The model has the attractive property that for a sufficiently large network, the degree distributions inside the communities and between the communities can be well approximated by a Poisson distribution. Later, we explain how to extend the approaches to a custom large graph with known in-community and between-community degree distributions.

### III. PROBABILITY-GENERATING FUNCTION FRAMEWORK IN A POISSON-DISTRIBUTED NETWORK

First, let us consider a network consisting of two communities that are Erdős–Rényi random graphs. For simplicity, we assume that both communities have  $\lambda_{\text{in}}$  expected number of internal edges. The edges between communities are also Poisson distributed with  $\lambda_{\text{out}}$  expected number of edges, where  $\lambda_{\text{in}} > \lambda_{\text{out}}$ . Meaning that, for example, a nodes in community 1 in-community degree is given by the random variable  $D_1^{(1)} \sim \text{Poi}(\lambda_{\text{in}})$  and a nodes between-community degree is given by the random variable  $D_2^{(1)} \sim \text{Poi}(\lambda_{\text{out}})$ . This corresponds to a *Stochastic Block Model* (SBM) [29].

A convenient way to describe the offspring distribution is through the use of *probability-generating functions* (PGFs), which maps all the probabilities of a discrete random variable onto a single power series. The goal of this section is to construct a PGF for the number of nodes active in each community at any time. We let  $N_1(t)$  be random variable for the number of active nodes in community 1 at generation  $t$  and  $N_2(t)$  be the random variable number of active nodes in community 2 at generation  $t$  (see Fig. 1b). We then introduce the probability generation function  $G_{\mathbf{N}(t)}$  for  $\mathbf{N}(t) = (N_1(t), N_2(t))$  that keeps track of the joint probabilities  $P[N_1(t) = n, N_2(t) = m]$  as

$$G_{\mathbf{N}(t)}(s_1, s_2) = \sum_{n=0}^{\infty} \sum_{m=0}^{\infty} P[N_1(t) = n, N_2(t) = m] s_1^n s_2^m, \quad (1)$$

where  $s_1$  and  $s_2$  are dummy variables in the power series for type 1 and type 2 offspring, respectively [22, 26]. Note that all PGFs will be labeled  $G(\vec{s})$ , which track the probabilities for the random variable  $\cdot$  with dummy variables  $\vec{s}$ .

To construct  $G_{\mathbf{N}(t)}$ , we begin by constructing the PGF for the offspring distribution generated by a single individual within the network. Let the random variable  $X_1^{(1)}$  denote the number of offspring of type 1 produced in the next generation by a single active individual of

type 1, and  $X_2^{(1)}$  the number of offspring of type 2 produced by a node of type 1. To clarify the notation, we note that the superscript identifies the type of the parent node (what community the parent is from) while the subscript points to the type of offspring produced (what community the offspring are in) — which is the same name convention used for the degree distributions. Then the PGF generating the offspring distribution produced by a single node of the first type,  $G_{\mathbf{X}^{(1)}}$ , is given by the bi-variate power series

$$G_{\mathbf{X}^{(1)}}(s_1, s_2) = \sum_{n=0}^{\infty} \sum_{m=0}^{\infty} P[X_1^{(1)} = n, X_2^{(1)} = m] s_1^n s_2^m, \quad (2)$$

where  $\mathbf{X}^{(1)} = (X_1^{(1)}, X_2^{(1)})$ . Similarly, the offspring distribution produced by a single node of type 2 is generated by

$$G_{\mathbf{X}^{(2)}}(s_1, s_2) = \sum_{n=0}^{\infty} \sum_{m=0}^{\infty} P[X_1^{(2)} = n, X_2^{(2)} = m] s_1^n s_2^m. \quad (3)$$

The PGFs  $G_{\mathbf{X}^{(1)}}$  and  $G_{\mathbf{X}^{(2)}}$  are easy to calculate if the in-community and between-community degree distributions of the networks are known. Moreover, if the number of offspring from types 1 and 2 are independent of each other, as is the case in the SBM, the PGF will factor into the product of two PGFs as follows

$$\begin{aligned} G_{\mathbf{X}^{(1)}}(s_1, s_2) &= G_{X_1^{(1)}}(s_1) G_{X_2^{(1)}}(s_2) \\ &= \sum_{n=0}^{\infty} P[X_1^{(1)} = n] s_1^n \sum_{m=0}^{\infty} P[X_2^{(1)} = m] s_2^m. \end{aligned} \quad (4)$$

In the SBM case, it is easy to obtain a closed-form expression for  $G_{\mathbf{X}^{(1)}}$  and  $G_{\mathbf{X}^{(2)}}$ . As the size of the network tends to infinity for an SBM, both in-community and between-community degree distributions will have a Poisson distribution with probabilities

$$\begin{aligned} P[D_1^{(1)} = k] &= \frac{\lambda_{\text{in}}^k e^{-\lambda_{\text{in}}}}{k!}, \quad \text{and} \\ P[D_2^{(1)} = k] &= \frac{\lambda_{\text{out}}^k e^{-\lambda_{\text{out}}}}{k!}. \end{aligned} \quad (5)$$

Now let us calculate the offspring distribution produced by a node of community 1, but note the same logic will apply to the nodes of the second community. First, we calculate the number of activation a node of community 1 produces inside its community. The probability of a node having  $k$  neighbours inside community 1 is given by Eqn. (5). Each of these neighbour nodes is activated independently with probability  $\rho$ , meaning that the probability of having  $x$  successfully activated nodes in community 1 from an active node with in-degree  $k$



is  $\frac{\lambda_{in}^k e^{\lambda_{in}}}{k!} \binom{k}{x} (1-\rho)^{k-x} (\rho)^x$ . Summing over all possible values of  $k$  yields the probability of having  $x$  activated offspring nodes inside community 1 as follows

$$P[X_1^{(1)} = x] = \frac{(\rho\lambda_{in})^x e^{-\rho\lambda_{in}}}{x!}, \quad (6)$$

which itself is Poisson distributed. Following the same argumentation, the probability of activation in community 2 produced by a node of community 1 is  $P[X_2^{(1)} = y] = \frac{(\rho\lambda_{out})^y e^{-\rho\lambda_{out}}}{y!}$ . The PGF generating offspring distribution produced by a node of community 1 is then

$$\begin{aligned} G_{\mathbf{X}^{(1)}}(s_1, s_2) &= \sum_{n=0}^{\infty} \frac{(\rho\lambda_{in})^n e^{-\rho\lambda_{in}}}{n!} s_1^n \sum_{m=0}^{\infty} \frac{(\rho\lambda_{out})^m e^{-\rho\lambda_{out}}}{m!} s_2^m \\ &= e^{\rho\lambda_{in}(s_1-1)} e^{\rho\lambda_{out}(s_2-1)}. \end{aligned} \quad (7)$$

Similarly, the PGF for the offspring distribution produced by an individual of type two is

$$G_{\mathbf{X}^{(2)}}(s_1, s_2) = e^{\rho\lambda_{out}(s_1-1)} e^{\rho\lambda_{in}(s_2-1)}. \quad (8)$$

The formulas (7) and (8) give us expressions for the PGFs generating the offspring distribution of each type of node for an SBM, and these are the main building blocks of our method. Once we derive them, calculating  $G_{\mathbf{N}(t)}$  becomes easy.

It is important to mention that in the general case of a non-Poissonian network, we will have to deal with a larger number of types in the MTBP because the seed node and the nodes activated in the subsequent generations will have different offspring distributions. Moreover the offspring distributions of nodes in the subsequent generations will depend on the way the node was

activated and we will need to account for the excess degree distributions when deriving the PGF [27]. The reason we start with a Stochastic Block Model is due to a convenient property of Poisson networks: their excess degree also follows a Poisson distribution.<sup>1</sup> This eliminates the necessity of accounting for the excess degree distribution and makes our final formulas more compact. However, we will have to return to the discussion of the excess degree distributions in Sec. IV where we extend our analysis to general networks.

After deriving  $G_{\mathbf{X}^{(1)}}$  and  $G_{\mathbf{X}^{(2)}}$  we can proceed with calculating the distribution of all active nodes at any given time step  $t$  as follows. The probability generating function  $G_{\mathbf{N}(t)}$  is calculated from the following function iteration:

$$G_{\mathbf{N}(t)}(s_1, s_2) = G_{\mathbf{N}(t-1)}(G_{\mathbf{X}^{(1)}}(s_1, s_2), G_{\mathbf{X}^{(2)}}(s_1, s_2)). \quad (9)$$

We have the probability generating function for the number of active nodes of type 1 and type 2 at time  $t - 1$ . Using this, we wish to see how many offspring we will have in the following generation using  $\mathbf{X}^{(1)}$  and  $\mathbf{X}^{(2)}$ . This characterisation of the branching process is called the forward approach in Ref. [28], in analogy with the forward Chapman-Kolmogorov equation of Markov processes. It is the common way in which one can derive the number of active nodes in a generation once we have obtained the offspring distributions for each type in MTBP. Refer to Caswell [26] for a derivation of this relationship. We set the initial condition  $G_{\mathbf{N}(0)}(s_1, s_2) = (s_1)^1 (s_2)^0$  corresponding to a single active individual in community 1 and none in community 2.

The utility of this PGFs formulation is that the PGF  $G_{\mathbf{N}(t)}$  contains information about all the probabilities of the number of active nodes in each community at any generation  $t$ , and these probabilities can be easily recovered from the PGF. By the definition, the joint probability  $P[N_1(t) = n, N_2(t) = m]$  is the corresponding derivative of  $G_{\mathbf{N}(t)}$ , as follows:

$$P[N_1(t) = n, N_2(t) = m] = \frac{1}{n!m!} \left[ \frac{\partial^n}{\partial s_1^n} \frac{\partial^m}{\partial s_2^m} (G_{\mathbf{N}(t)}(s_1, s_2)) \right]_{(s_1=0, s_2=0)}. \quad (10)$$

However, numerical differentiation of PGFs can prove to be unstable, especially for higher-order derivatives.

Thus, in practice we use the discrete Fourier transform to evaluate probabilities for the first  $K$  values for  $N_1(t)$  and  $N_2(t)$  as follows [23, 30, 31]:

<sup>1</sup> The degree distribution of a Poissonian network is  $D(k) = e^{-\langle k \rangle} \langle k \rangle^k / k!$ , where  $\langle k \rangle$  is the mean-degree. The excess degree distribution,  $\tilde{D}(k)$ , by definition is given by  $\tilde{D}(k) =$

$D(k+1)(k+1)/\langle k \rangle$ . The excess degree distribution for the Poissonian network is then  $\tilde{D}(k) = e^{-\langle k \rangle} \langle k \rangle^k / k!$ , which is exactly the degree distribution  $D(k)$  [27].

$$P[N_1(t) = n, N_2(t) = m] \approx \frac{1}{K^2} \sum_{k_1=0}^{K-1} \sum_{k_2=0}^{K-1} G_{\mathbf{N}(t)}(e^{2\pi i k_1/K}, e^{2\pi i k_2/K}) e^{2\pi i n k_1/K} e^{2\pi i m k_2/K}. \quad (11)$$

How to make the transition from Eqn. (10) to (11) is explained in App. A.

To obtain the probability distribution of number of active nodes in each of the communities separately,  $P[N_1(t) = n]$  and  $P[N_2(t) = m]$ , we simply marginalise the probabilities in the community that is not of interest. Thus, the probability  $P[N_1(t) = n]$  will be recovered from  $G_{\mathbf{N}(t)}(s_1, 1)$ , while the probability  $P[N_2(t) = m]$  will be recovered from  $G_{\mathbf{N}(t)}(1, s_2)$ , e.g.,

$$P[N_1(t) = n] \approx \frac{1}{K} \sum_{k=0}^{K-1} G_{\mathbf{N}(t)}(e^{2\pi i k/K}, 1) e^{2\pi i n k/K}. \quad (12)$$

Moreover, to obtain the probability of the total number of active nodes,  $P[N_1(t) + N_2(t) = n]$ , we make the substitution  $s_1 = s$ ,  $s_2 = s$  and apply the discrete Fourier transform to  $G_{\mathbf{N}(t)}(s, s)$ . For a more detailed explanation of how to recover the probabilities from  $G_{\mathbf{N}(t)}$  see App. B.

In summary, using the recursive Eqn. (9), together with PGFs for the offspring distributions (7) and (8) we can determine  $G_{\mathbf{N}(t)}$  for any given generation. Using this we can then obtain some quantities of interest like the extinction probabilities, hazard function and the introduction probabilities (which is the focus on the following sections). Additionally, once we have  $G_{\mathbf{N}(t)}$ , we compute the actual probabilities with the use of discrete Fourier transform (11). Once we have the probability distributions for the number of active nodes of each type at any time point, we possess complete knowledge about the process.

### A. Extinction probability and hazard function

Our PGF approach allows us to straightforwardly calculate common survival analysis probabilities, such as the extinction probability and hazard function. Let us calculate the *extinction probability*, the probability that the process is extinct at generation  $t$  in both communities,  $q(t) = P[N_1(t) = 0, N_2(t) = 0]$ . From the properties of PGFs, it follows that

$$\begin{aligned} q(t) &= P[N_1(t) = 0, N_2(t) = 0] \\ &= \sum_{n=0}^{\infty} \sum_{m=0}^{\infty} P[N_1(t) = n, N_2(t) = m] (0)^n (0)^m \quad (13) \\ &= G_{\mathbf{N}(t)}(0, 0). \end{aligned}$$

We can also straightforwardly evaluate the probability of the process being extinct at generation  $t$  only in com-

munity 1 or 2, respectively as

$$\begin{aligned} q_1(t) &= P[N_1(t) = 0] = G_{\mathbf{N}(t)}(0, 1) \text{ and} \\ q_2(t) &= P[N_2(t) = 0] = G_{\mathbf{N}(t)}(1, 0). \end{aligned} \quad (14)$$

With a bit more effort, we can compute the *hazard function*, which is the probability that the process is extinct in a community at time  $t$  given that it is not extinct at  $t-1$ , while possibly still spreading in the other community. We start with the hazard function for community 1,  $h_1(t) = P[N_1(t) = 0 | N_1(t-1) + N_2(t-1) > 0]$ . This can be expressed as

$$\begin{aligned} h_1(t) &= 1 - \sum_{k=1}^{\infty} P[N_1(t) = k | N_1(t-1) + N_2(t-1) > 0] \\ &= 1 - \frac{\sum_{k=1}^{\infty} P[N_1(t) = k] s^k}{P[N_1(t-1) + N_2(t-1) > 0]}. \end{aligned} \quad (15)$$

Noting that  $\sum_{k=1}^{\infty} P[N_1(t) = k] = 1 - G_{\mathbf{N}(t)}(0, 1)$  and  $P[N_1(t-1) + N_2(t-1) = 0] = G_{\mathbf{N}(t-1)}(0, 0)$  we obtain

$$h_1(t) = \frac{G_{\mathbf{N}(t)}(0, 1) - G_{\mathbf{N}(t-1)}(0, 0)}{1 - G_{\mathbf{N}(t-1)}(0, 0)}, \quad (16)$$

which is the hazard function for community 1. In the same way, the hazard function for the second community is

$$h_2(t) = \frac{G_{\mathbf{N}(t)}(1, 0) - G_{\mathbf{N}(t-1)}(0, 0)}{1 - G_{\mathbf{N}(t-1)}(0, 0)}, \quad (17)$$

while the hazard function for the entire network is

$$h(t) = \frac{G_{\mathbf{N}(t)}(0, 0) - G_{\mathbf{N}(t-1)}(0, 0)}{1 - G_{\mathbf{N}(t-1)}(0, 0)}. \quad (18)$$

In Fig. 2a) we show the extinction probability distribution for the entire network and the distributions for each community calculated using Eqns. (13) and (14). It compares the analytical results with branching process simulations where  $\lambda_{in} = 8$ ,  $\lambda_{out} = 2$  and  $\rho = 0.06$ . The hazard functions for the SBM and each community are shown in Fig. 2b) and we note the excellent agreement between our simulation and theory curves. For our numerical simulations, we use branching process simulations repeated  $5 \times 10^4$  times and we compute all distributions as averages across these simulations. In App. C we demonstrate that the branching process simulation agrees with network-based simulations performed on actual networks with a sufficiently

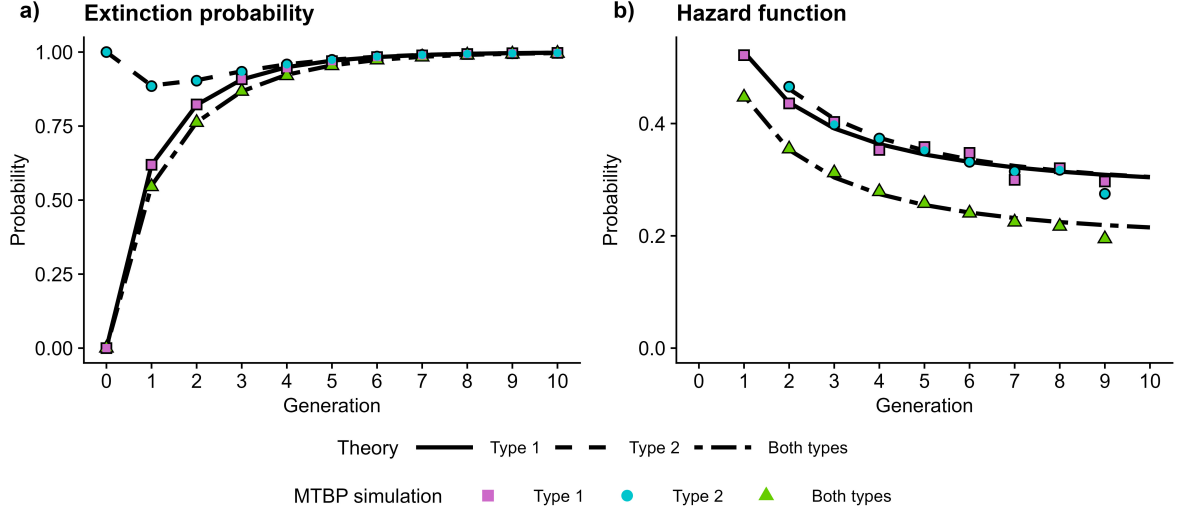


Figure 2: a) Extinction probability for Stochastic Block Model; b) Hazard function for Stochastic Block Model. Here,  $\lambda_{\text{in}} = 8$ ,  $\lambda_{\text{out}} = 2$  and  $\rho = 0.06$ . For numerical simulations, we use branching process simulations with averaging across  $5 \times 10^4$  simulations. The hazard function starts in generation 1 (not 0) as the probability of survival until generation 0 is not defined.

large number of nodes. With both the extinction probabilities and hazard function to hand, we next show that it is possible to construct a community-specific hazard function. This will be an important building block in constructing the probability of reintroducing activations into a community where it had no active nodes in the previous generation.

### 1. Community specific hazard function

We can now calculate what we call the *community specific hazard function*,  $\tilde{h}_1(t)$  and  $\tilde{h}_2(t)$ . They are hazard functions specified for each community on non-extinction in community 1 or community 2 in the previous time step, i.e.,  $\tilde{h}_1(t) = P[N_1(t) = 0 | N_1(t-1) > 0]$  and  $\tilde{h}_2(t) = P[N_2(t) = 0 | N_2(t-1) > 0]$ . In contrast,  $h_1(t)$  in the last section was the hazard function for community 1 conditioned on the joint non-extinction of the process in the previous time step (i.e.,  $N_1(t-1) = 0$  and  $N_2(t-1) > 0$ ). This can be useful if we care more about when the process stops in a specific community disregarding whether it is still going on in the other one. To derive the expression for  $\tilde{h}_2(t)$  we introduce the random variables  $Y_1(t)$  and  $Y_2(t)$  such that  $P[Y_1(t) = k] = P[N_1(t) = k | N_1(t-1) > 0]$ . We note that  $Y_1(s)$  is the PGF for the number of active nodes at time  $t$ , conditional on the process being non-zero in community 1. Then  $G_{Y_1(t)}(s_1, s_2)$  is easily calculated

from  $G_{N(t)}(s_1, s_2)$ , as follows

$$G_{Y_1(t)}(s_1, s_2) = \frac{G_{N(t)}(s_1, s_2) - G_{N(t)}(0, s_2)}{1 - G_{N(t)}(0, 1)}. \quad (19)$$

To see this, write out the power series of  $G_{N(t)}(s_1, s_2)$  and subtract the terms corresponding to  $G_{N(t)}(0, s_2)$ , which then is normalised. We can now note a connection between our desired probability  $\tilde{h}_1(t)$  and  $G_{Y_1(t-1)}$ . The function  $G_{Y_1(t-1)}$  tracks the probabilities for the number of active nodes at time  $t-1$  given the process is not extinct in community 1. If we find the number of offspring of the active nodes from the  $t-1$  generation, we can arrive at the PGF for number of active nodes in generation  $t$  conditioned on the process not being extinct in generation  $t-1$ . This is given by:

$$G_{Y_1(t-1)}(G_{\mathbf{X}^{(1)}}(s_1, s_2), G_{\mathbf{X}^{(2)}}(s_1, s_2)). \quad (20)$$

This gives us a way to express the community-specific hazard probability for community 1. Then by calculating the probability of extinction in community 1 (setting  $s_1 = 0$ ) and marginalising over community 2 (by setting  $s_2 = 1$ ) in generation  $t$ , we obtain  $\tilde{h}_1(t)$ , as required:

$$\begin{aligned} \tilde{h}_1(t) &= G_{Y_1(t-1)}(G_{\mathbf{X}^{(1)}}(0, 1), G_{\mathbf{X}^{(2)}}(0, 1)) \\ &= \frac{G_{N(t)}(0, 1) - G_{N(t-1)}(0, G_{\mathbf{X}^{(2)}}(0, 1))}{1 - G_{N(t-1)}(0, 1)}. \end{aligned} \quad (21)$$

Similarly, the community-specific hazard probabilities for community 2,  $\tilde{h}_2(t)$ , can be derived through an analogous process. It is important to note that we can arrive at all these expressions via simple function iteration

followed by the appropriate substitutions of zeros and ones into the dummy variables  $s_1$  and  $s_2$ . Equation (21) allows us to finally arrive at an important quantity of interest, the probability of information spreading between communities, which we derive in the next section.

### B. Probability of information travel between communities

When studying the spread of information or disease on a network with communities, a crucial question arises: What is the probability of infection spreading to another community? Here we show how to calculate this probability with our framework. Let  $r_1(t) = P[N_1(t) > 0 | N_1(t-1) = 0]$  be the probability of infection in the first community at time  $t$ , given no infected nodes in that community at time  $t-1$ , which we

will call the *introduction probability* for community 1. Care must be taken in noting what  $r_1(t)$  is; it measures the probability of seeing an activated node in community 1, maybe for the first time, but also for the second time, third time, etc. All we know is that there was no infected (active) node in the community in the previous time step. It can be expressed as

$$\begin{aligned} r_1(t) &= 1 - P[N_1(t) = 0 | N_1(t-1) = 0] \\ &= 1 - \phi_1(t), \end{aligned} \quad (22)$$

where we will call  $\phi_1(t) = P[N_1(t) = 0 | N_1(t-1) = 0]$  the probability of continued extinction for community 1. Deriving an expression for  $\phi_1(t)$  is straightforward by first expanding  $q_1(t)$ , where we condition on extinction and non-extinction in the previous time step in community 1. Once this is done we can then match terms to quantities we have already derived in previous sections:

$$\begin{aligned} q_1(t) &= \underbrace{P[N_1(t) = 0 | N_1(t-1) = 0]}_{\phi_1(t)} \times \underbrace{P[N_1(t-1) = 0]}_{q_1(t-1)} + \underbrace{P[N_1(t) = 0 | N_1(t-1) > 0]}_{\tilde{h}_1(t)} \times \underbrace{P[N_1(t-1) > 0]}_{1 - q_1(t-1)} \\ &= \phi_1(t)q_1(t-1) + \tilde{h}_1(t)[1 - q_1(t-1)]. \end{aligned} \quad (23)$$

Then Eqn. (23) can easily be rearranged to isolate  $\phi_1(t)$  yielding

$$\phi_1(t) = \frac{q_1(t) - \tilde{h}_1(t)[1 - q_1(t-1)]}{q_1(t-1)}, \quad (24)$$

where  $\tilde{h}_1(t)$  and  $q_1(t)$  are calculated by Eqn. (21) and Eqn. (14). Using Eqn. (22) we can derive the reintroduction probability for community 1 as  $r_1(t) = 1 - \phi_1(t)$ . The same logic holds when deriving expressions for  $\phi_2(t)$  and  $r_2(t)$  as we have used above.

We plot the probabilities of introduction and reintroduction for any time point in Fig. 3a) and we observe an excellent agreement with the simulated data. Note that the probability of reintroduction is not defined for the first generation as the process is still alive at the previous generation, i.e., generation zero.

### C. Cascade size distribution

In this section, we calculate the overall size of outbreaks, i.e., the cascade size distribution, with our

framework. The cascade size distribution is also referred to as the total progeny distribution of a seed within the literature on branching processes [28]. This cascade size distribution can simply be found by introducing a counter type into our multi-type branching process that tracks the total number of active nodes that have been created for each community.<sup>2</sup> To achieve this, first let  $C_1$  be a random variable tracking the total number of active nodes in a cascade, such that  $P[C_1(t) = k] = P[\sum_i^t N_1(i) = k]$  and  $C_2(t)$  is defined similarly as  $P[C_2(t) = k] = P[\sum_i^t N_2(i) = k]$ . The probability generation function that maps the joint probability distribution of variables  $N_1, N_2, C_1$  and  $C_2$  will be

<sup>2</sup> The authors found the idea of using a counter in this manner in Ref. [32], where it was introduced as a means of calculating

expected population size in a MTBP.

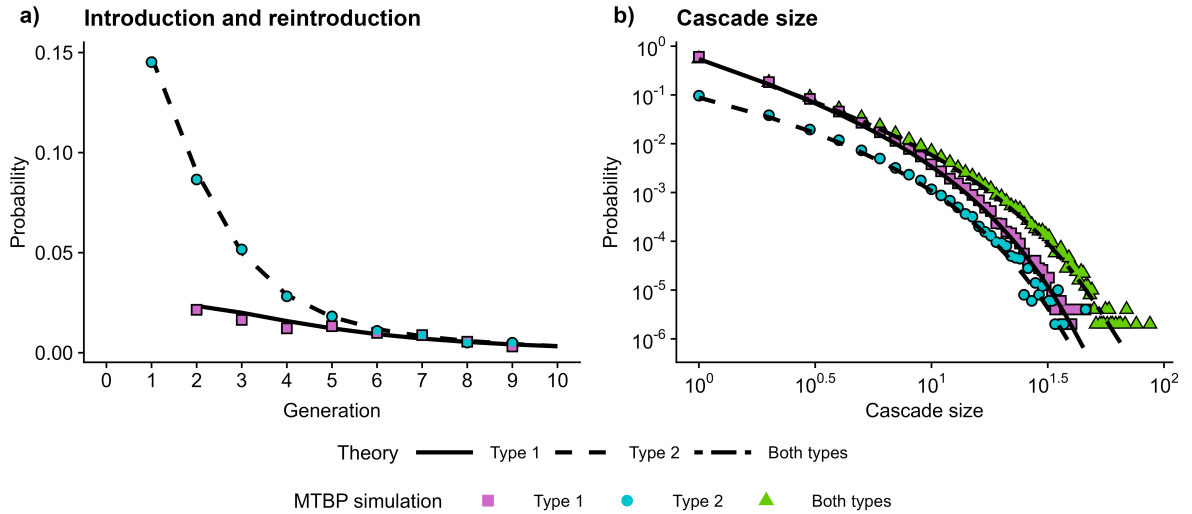


Figure 3: a) Probability of infection spreading to community 2 and the probability of reintroduction back to community 1 for SBM. For numerical simulations, we use branching process simulations where we average across  $5 \times 10^5$  simulations. Here,  $\lambda_{\text{in}} = 8$ ,  $\lambda_{\text{out}} = 2$  and  $\rho = 0.08$ ; b) Cascade size distribution for SBM. Here,  $\lambda_{\text{in}} = 8$ ,  $\lambda_{\text{out}} = 2$  and  $\rho = 0.06$ .

$$G_{\mathcal{C}(t)}(s_1, s_2, c_1, c_2) = \sum_{i,j,k,l} P[N_1(t) = i, N_2(t) = j, C_1(t) = k, C_2(t) = l] s_1^i s_2^j c_1^k c_2^l. \quad (25)$$

Here dummy variables  $c_1$  and  $c_2$  will track the cumulative number of active nodes in communities 1 and 2, respectively. The PGF  $G_{\mathcal{C}(t)}$  is effectively an extension of  $G_{N(t)}$ , which includes two new counter types that

track the number of active nodes in each community. Just as we had a recursive relationship  $G_{N(t)}$  given by Eqn. (9), we have a recursive relationship for  $G_{\mathcal{C}(t)}$  given by

$$G_{\mathcal{C}(t)}(s_1, s_2, c_1, c_2) = G_{\mathcal{C}(t-1)}(G_{\mathbf{X}^{(1)}}(\overbrace{s_1 c_1, s_2 c_2}^{\text{When a type-1 node is created a type-1 counter is created also.}}, G_{\mathbf{X}^{(2)}}(s_1 c_1, s_2 c_2), \underbrace{c_1, c_2}_{\text{Number of counters persist from } t-1 \text{ to } t.}) \quad (26)$$

Here the counters for the number of nodes in community 1 or 2 are tracked by the dummy variables  $c_1$  and  $c_2$ . Then each counter type always produce exactly one copy of themselves between generations, thus accounting for the total cascade size. The initial condition is then given as  $G_{\mathcal{C}(0)}(s_1, s_2, c_1, c_2) = s_1 c_1$ , where we have one active node in community one ( $s_1$ ) and a counter for that node ( $c_1$ ).

As we are interested in the total cascade size, we substitute  $c_1 = c$  and  $c_2 = c$  in  $G_{\mathcal{C}(t)}(1, 1, c, c)$ . We then marginalize  $s_1$  and  $s_2$  in Eqn. (25) to calculate the actual probabilities  $P[C_1(t) + C_2(t) = n]$ , which is a uni-

variate PGF. The probability distribution can then be estimated from the univariate PGF using the inverse fast Fourier transform to obtain the cascade size distribution as discussed in App B. Moreover, in the same manner, functions  $G_{\mathcal{C}(t)}(1, 1, c, 1)$  and  $G_{\mathcal{C}(t)}(1, 1, 1, c)$  can yield the probability distribution for cascade sizes in community one and community two, respectively. As Fig. 3b) illustrates, our framework accurately estimates the expected cascade sizes not only for the entire network but also for each community individually.

#### IV. EXTENDING THE PGF FRAMEWORK TO A GENERAL NETWORK WITH COMMUNITIES

In this section, we extend the analysis presented in Sec. III to a broader class of networks with community structure, where their degree distributions do not necessarily follow the Stochastic Block Model, i.e., the in- and between community degree distribution are not Poisson. While the networks constituting communities can be general, they are required to have a local tree-like structure and be well-described via the configuration model. In principle, it is possible to relax these assumptions, but this is left to future work.

Incorporating networks with a general degree requires careful consideration of the origin of node activation — whether from within or outside its own community. This in turn, will lead to the use of excess offspring distributions. Below, we explain how to incorporate this into our framework. As in the previous section, the first step is to derive the offspring distributions for each type of node we track. Let us start by calculating the offspring distribution for the seed node in community 1. For our framework to work we need to know (or be able to extract) the in-community degree of each node,  $D_1^{(1)}$  and  $D_2^{(2)}$ , and the between-community degree of each node,  $D_2^{(1)}$  and  $D_1^{(2)}$ . We then construct the PGFs corresponding degree distributions, e.g.,

$$G_{D_1^{(1)}}(s) = \sum_{k=1}^{\infty} P[D_1^{(1)} = k] s^k, \quad (27)$$

and  $G_{D_2^{(1)}}(s) = \sum_{k=1}^{\infty} P[D_2^{(1)} = k] s^k.$

When we have this, we proceed with calculating the PGF for the offspring distribution as follows. Under the ICM, the probability that a single node, who is in contact with an active node, will become active themselves is defined by the PGF for a Bernoulli distribution  $G_I(s) = 1 - \rho + \rho s$ , where  $I \sim Ber(\rho)$ . The number of active individuals in- and between-community one defines randomly stopped sums  $X_1^{(1)} = \sum_{k=0}^{D_1^{(1)}} I$  and  $X_2^{(1)} = \sum_{k=0}^{D_1^{(2)}} I$ , respectively. With the PGF for the randomly stopped sum of the offspring distributions can be written compactly as

$$G_{X_1^{(1)}}(s) = G_{D_1^{(1)}}(G_I(s)), \quad (28)$$

and  $G_{X_2^{(1)}}(s) = G_{D_2^{(1)}}(G_I(s)).$

This gives us, respectively, the probability generating functions for the offspring distribution from a randomly active node in community 1 inside its community and between communities [33]. Similarly, if we

start in community 2, the offspring distributions for the seed node will be  $G_{X_2^{(2)}}(s) = G_{D_2^{(2)}}(G_I(s))$  and  $G_{X_1^{(2)}}(s) = G_{D_1^{(2)}}(G_I(s))$ . PGFs are particularly useful when dealing with randomly stopped sums, see Ref. [33] for a brief useful introduction. In fact, the reader might find it interesting to note that Eqns. (7) and (9) are both randomly stopped sums of the same form as Eqn. (28).

Now, let us consider what happens when the activations spread beyond the seed generation. According to ICM, a node cannot be activated again once it has been activated in a previous time step. If we have an active node, who was activated by a neighbour in the previous generation, the number of inactive (susceptible) nodes that can then go on to be activated differs from the seed generation. To account for this, we need to use the appropriate excess degree distribution.

Mathematically, the relationship between the PGF of a distribution and its excess distribution is an elegant and simple one [27]. If we have a PGF for the offspring distribution, with associated random variable  $X_1^{(1)}$  and PGF  $G_{X_1^{(1)}}(s)$ , its excess offspring PGF will be given by

$$G_{\tilde{X}_1^{(1)}}(s) = \frac{G'_{X_1^{(1)}}(s)}{G'_{X_1^{(1)}}(0)}. \quad (29)$$

To account for this in our multi-type branching process, we need to also consider where a node activation originated from — either by another node from their community or from outside their community, as illustrated in Fig. 4. Consider an active node in community 1 after generation  $t = 0$ . This node could have been activated in two ways:

- (1) If it was activated from inside its own community, then to correctly track activations from it, we need to use the excess offspring distribution for community 1, with associated random variable  $\tilde{X}_1^{(1)}$ , (as we have used up one possible link that the activations could travel down), and the offspring distribution for between-communities, with associated random variable  $X_2^{(1)}$ , (as we have not used up any edges between communities from which activations could traverse).
- (2) If it was activated from outside its own community (by a node in community 2), then to correctly track activations from it, we need to use the offspring distribution for community 1, with associated random variable  $X_1^{(1)}$ , (as we have not used up a possible edge that the activations could travel down inside its own community), and the excess offspring distribution for between-communities, with associated random variable  $\tilde{X}_2^{(1)}$ , (as we have used up an edge

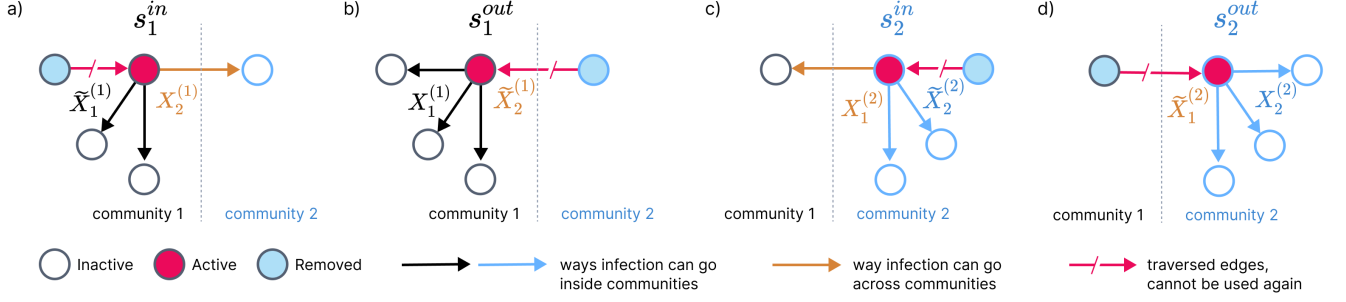


Figure 4: Schematic illustrating four types of offspring tracking in the model: a)  $s_1^{in}$  represents offspring in community 1 produced by traversing the edge within community 1. It produces  $\tilde{X}_1^{(1)}$  and  $X_2^{(1)}$  offspring in the next time step; b)  $s_1^{out}$  is offspring in community 1 produced by traversing the edge from community 2, producing  $X_1^{(1)}$  and  $\tilde{X}_2^{(1)}$  offspring in the next time step; c)  $s_2^{in}$  is offspring in community 2 produced by traversing the edge within community 2. It creates  $X_1^{(2)}$  and  $\tilde{X}_2^{(2)}$  offspring in the next time step; d)  $s_2^{out}$  is offspring in community 2 produced by traversing the edge from community 1. It creates  $\tilde{X}_1^{(2)}$  and  $X_2^{(2)}$  offspring in the next time step. The red arrow represents the edge through which the node was infected. This edge cannot be used again, so we use the excess degree distribution for the communities with a traversed edge. Black, blue and yellow arrows show the ways that infection can proceed in the next generation.

between communities from which activations could traverse).

To track each of these cases for community 1 we introduce two types, each representing where a node in community 1 was activated from. The same logic holds for community 2, therefore, we now must keep track of four distinct types of offspring produced, which leads us, as illustrated in Fig. 4, to a 4-type branching process. The corresponding PGFs will use dummy variables  $s_1^{in}$  to track active nodes in community 1 that were activated through a link inside community 1, and  $s_1^{out}$  for activations through links from community 2. Likewise, the offspring in community 2 obtained from travelling the edge inside and outside community 2 will be tracked by  $s_2^{in}$  and  $s_2^{out}$ , respectively. Each of these types will have their own offspring distributions and probability-generating functions, which are shown in Tab. I.

The updated notation allows us to specify our multivariate PGFs for the offspring that each type can have. For example, an active node in community 1, where it was activated from within its own community in the previous generation, will use the excess offspring distribution for its own community, with associated random variable  $\tilde{X}_1^{(1)}$ , and offspring distribution for between the communities, with associated random variable  $X_2^{(1)}$ . This leads, naturally, to the PGF for the

number of offspring defined by

$$G_{\mathbf{X}_{in}^{(1)}}(s_1^{in}, s_2^{out}) = \overbrace{G_{\tilde{X}_1^{(1)}}(s_1^{in}) G_{X_2^{(1)}}(s_2^{out})}^{\text{Note use of excess offspring PGF due to parent coming from community 1.}}. \quad (30)$$

Offspring PGF due to parent coming from community 1.

Equation (30) holds as we are treating the degree inside and outside of a community as independent of each other, and the PGF for the sum of independent random variables can be found by taking the product of their PGFs.

Following the same logic as for the derivation of Eqn. (30), we write the expressions for the PGFs for offspring distributions produced by each type of nodes by replacing the degree distributions with their corresponding excess degree distributions where necessary. We obtain

$$\begin{aligned} G_{\mathbf{X}_{out}^{(1)}}(s_1^{in}, s_2^{out}) &= G_{X_1^{(1)}}(s_1^{in}) G_{\tilde{X}_2^{(1)}}(s_2^{out}), \\ G_{\mathbf{X}_{in}^{(2)}}(s_2^{in}, s_1^{out}) &= G_{\tilde{X}_2^{(2)}}(s_2^{in}) G_{X_1^{(2)}}(s_1^{out}), \\ G_{\mathbf{X}_{out}^{(2)}}(s_2^{in}, s_1^{out}) &= G_{X_2^{(2)}}(s_2^{in}) G_{\tilde{X}_1^{(2)}}(s_1^{out}). \end{aligned}$$

See Tab. I for the summary of the PGFs for the offspring distributions.

After defining the PGFs for the offspring distributions generated by a single node of each type, we can apply the same approach as in Sec. III while keeping track of additional random variables. We define the PGF generating the number of active nodes of all types for each generation as

PGF	What it generates
$G_{\mathbf{X}^{(1)}}$	Offspring produced by a seed node.
$G_{\mathbf{X}_{in}^{(1)}}$	Offspring produced by a node from community 1 who was activated by traversing an edge inside community 1.
$G_{\mathbf{X}_{out}^{(1)}}$	Offspring produced by a node from community 1 who was activated by traversing an edge coming from community 2.
$G_{\mathbf{X}_{in}^{(2)}}$	Offspring produced by a node from community 2 who was activated by traversing an edge inside community 2.
$G_{\mathbf{X}_{out}^{(2)}}$	Offspring produced by a node from community 2 who was activated by traversing an edge coming from community 1.

Table I: Summary of probability-generating functions generating offspring distributions.

$$G_{\mathcal{N}(t)}(s_1^{in}, s_1^{out}, s_2^{in}, s_2^{out}) = \sum_{k,l,m,n} P[\mathcal{N}_1^{in}(t) = k, \mathcal{N}_1^{out}(t) = l, \mathcal{N}_2^{in}(t) = m, \mathcal{N}_2^{out}(t) = n] (s_1^{in})^k (s_1^{out})^l (s_2^{in})^m (s_2^{out})^n;$$

here  $\mathcal{N}(t) = (\mathcal{N}_1^{in}(t), \mathcal{N}_1^{out}(t), \mathcal{N}_2^{in}(t), \mathcal{N}_2^{out}(t))$  is a random variable for numbers of active nodes of each type at generation  $t$ . We use  $\mathcal{N}(t)$  instead of  $N(t)$  to

differentiate it from the Poisson networks case. As before, in Sec. III, the PGF for  $\mathcal{N}(t)$  is calculated from the self-contained formula

$$G_{\mathcal{N}(t)}(s_1^{in}, s_1^{out}, s_2^{in}, s_2^{out}) = G_{\mathcal{N}(t-1)} \left( G_{\mathbf{X}_{in}^{(1)}}, G_{\mathbf{X}_{out}^{(1)}}, G_{\mathbf{X}_{in}^{(2)}}, G_{\mathbf{X}_{out}^{(2)}} \right), \quad (31)$$

We note that if we have a single seed in community 1 then generation 1 will have a slightly different PGF, as no spreading has taken place to require the use of an excess degree distribution. Therefore  $G_{\mathcal{N}(1)}(s_1^{in}, s_1^{out}, s_2^{in}, s_2^{out}) = G_{\mathbf{X}_1^{(1)}}(s_1^{in}) G_{\mathbf{X}_2^{(1)}}(s_2^{out})$ .

In Sec. III A and Sec. III B, we derived many characteristic distributions of interest for the Stochastic Block Model. It is important to note that these formulas still hold for  $G_{\mathcal{N}(t)}(s_1^{in}, s_1^{out}, s_2^{in}, s_2^{out})$ . Moreover, as we are only interested in the distribution of the total number of active nodes in community 1 or community 2, regardless of where they were activated from, we can easily recover these distributions by noting that setting  $s_1^{in}$  and  $s_1^{out}$  equal to  $s_1$  and  $s_2^{in}$  and  $s_2^{out}$  equal to  $s_2$  reduces  $G_{\mathcal{N}(t)}$  to  $G_{\mathbf{N}(t)}$ , i.e.,

$$G_{\mathcal{N}(t)}(s_1, s_1, s_2, s_2) = G_{\mathbf{N}(t)}(s_1, s_2). \quad (32)$$

With this formula in mind, we can now apply all the formulas derived for the statistical characteristics for the Stochastic Block Model in Sec. III to calculate the same characteristics for a general network of interest. In the following section, we will apply our method to a network with heavy-tailed degree distribution to illustrate our framework for a general network.

#### A. Application of pgf framework to a log-normal network with community structure

We now focus on a more complex and realistic structure than the simple SBM studied in Sec. III. We use a network with a discrete log-normal degree distribution as it can exhibit heavier tails than the Poisson distribution, yet it can be easily adjusted to avoid excessively broad distributions. This is important for computational reasons, the broader the degree distribution, the more terms required in the sums defining the PGFs. Additionally, we set the number of between-community edges to be small, with either no connections or only one connection per node between communities. Both communities will be of the same size. This leaves our multi-type branching process description in a general form, allowing for a ‘plug-and-play’ set-up if one wishes to explore other network structures.

To construct the required PGF we first need the in- and between-community degree distributions. To extract these, we simulate two networks of 5000 nodes, each with a log-normal distribution internally with  $\mu_1 = 0.85$  and  $\sigma_1 = 0.4$  ( $\mu_2 = 1.8$  and  $\sigma_2 = 0.4$ ) for community 1 (and community 2, respectively). As the log-normal is a continuous distribution, the generate numbers are real-valued no integer valued, therefore, we apply the ceiling function to these sampled values.



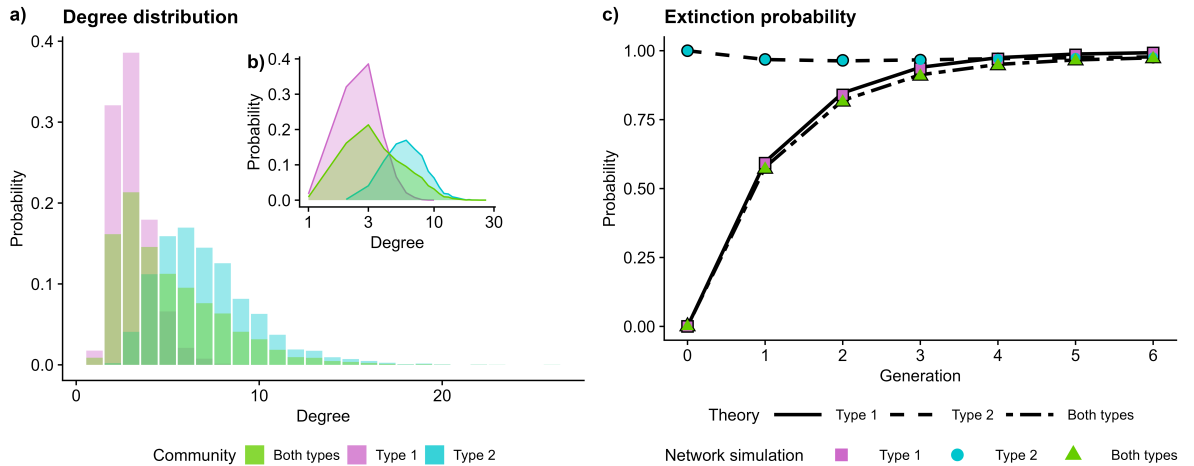


Figure 5: a) Degree distribution for our example log-normal network. Nodes in community 1 have an average degree of  $\approx 3$ , nodes in community 2 have an average degree of  $\approx 7$  and the average degree for a randomly selected node on the network is  $\approx 5$ . These degree distributions also include the cross community edges; b) Degree distribution for our example log-normal network where the x axis is on a log scale; c) Extinction probability for log-normal network. Here,  $\rho = 0.16$ .

This yields an internal degree structure where the average degree of nodes in community 1 is approximately 3, and the average degree of nodes in community 2 is approximately 7. Figure 5a) shows the degree distribution for our example network. With these distributions, we can formulate the required PGFs  $G_{X_1^{(1)}}$  and  $G_{X_2^{(2)}}$ , and then construct the excess offspring distributions  $G_{\tilde{X}_1^{(1)}}$  and  $G_{\tilde{X}_2^{(2)}}$ .

To generate community structure we add edges between community 1 and community 2 in the following way. We randomly select  $n_e$  nodes from community 1 and  $n_e$  nodes from community 2, and connect each node across the communities. The value of  $n_e$  is set to be 100. The probability of a node having a cross-community edge is then given by probability  $p_e = n_e/5000 = 0.02$ . As both communities are of the same size, this yields the same between-community degree distribution, which will have PGF  $G_I(s) = 1 - p_e + p_e s$ , leading to the between-community offspring distributions

$$\begin{aligned} G_{X_2^{(1)}}(s) &= G_{X_1^{(2)}}(s) = 1 - p_e + p_e(G_I(s)) \\ &= 1 - p_e + p_e(1 - \rho + \rho s). \end{aligned}$$

We can easily show that the excess offspring distributions for between-community spread are given by  $G_{\tilde{X}_2^{(1)}}(s) = G_{\tilde{X}_1^{(2)}}(s) = s^0 = 1$ . This means that, for example, if a node in community 1 was infected by an edge emanating from community 2 it is certain to have no other edges connecting to community 2 (as we have used the only edge to activate it). Now that we have the four probability generation functions, we can iterate them to find the probability generation function for the

number of active nodes at time  $G_{\mathcal{N}(t)}$ .

Once we constructed  $G_{\mathcal{N}(t)}$ , we can proceed to calculate characteristics of interest, such as cascade sizes and extinction probabilities. In Fig. 5b) we show the extinction probabilities calculated for the log-normal network using equations (13) and (14). We observe excellent agreement with the simulated distributions. In the next section, we focus on the cascade size distribution.

## B. The community seeding effect on cascade sizes

This section will focus on how the community structure, where an infection is seeded, changes the observed cascade size distribution. Figure 6 shows how the cascade size distribution changes for a range of infection ( $\rho$ ) parameters when seeded in different communities, leaving the cross-community connection probability,  $p_e$ , fixed at 0.02. We see that if we seed the branching process in community 1, which has a lower average degree, the probability of producing larger cascades is lower than if we seed initially in community 2 (which has a larger average degree). We can also note that our framework accurately captures this effect. See App. D for a wider parameter sweep and for how these values change when we also vary the between-community connection probability  $p_e$ .

Next, we would like to isolate the effect of the community structure from the degree structure. To achieve this we compare the cascade dynamics on the network with communities to the cascades on the network with

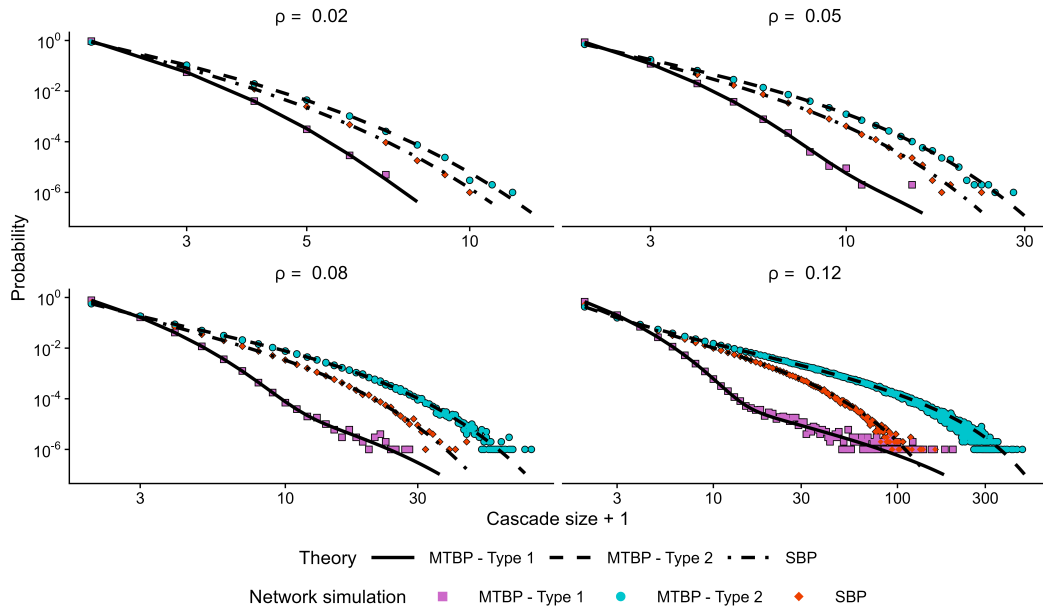


Figure 6: Cascade size distribution changes for a range of infection ( $\rho$ ) parameters when seeded in different communities, leaving the cross-community connection probability,  $p_e$ , fixed at 0.02. Each community has 5000 nodes, totalling 10000 nodes in the network. The internal connections in community 1 and community 2 are those stated in Fig. 5. Lines represent theory curves, and the points represent the results of  $N_{sim} = 10^6$  Monte Carlo simulations of the ICM model on the network. Note that the middle dot-dashed line is for the corresponding simple branching process (which does not take into account community structure).

the same degree distribution but without community structure. To construct such a network, we take the network with community structure and perform a degree-preserving randomisation. This removes the community structure but preserves the degree structure as required. We then simulate the ICM on this network to compare it to our network with community structure.

Moreover, we can easily construct a branching processes tracking diffusion on such a network and compare its prediction to the prediction of the multi-type branching process developed in this paper. To do this, we need to construct a PGF for  $\mathcal{N}_s(t)$ , the number of active nodes at time  $t$  in a network without communities. The degree of a randomly chosen node from the network, denoted with the random variable  $D_T$ , is given by

$$D_T = \frac{1}{2} \overbrace{\left( D_1^{(1)} + D_2^{(1)} \right)}^{\text{The total degree of nodes in community 1.}} + \frac{1}{2} \overbrace{\left( D_1^{(2)} + D_2^{(2)} \right)}^{\text{The total degree of nodes community 2.}}. \quad (33)$$

This arises as the communities have equal size. if we randomly select a node from the entire network then we have a 50% chance of selecting a node from community 1 or 2. The probability generating function for the number of offspring of a randomly selected node in a

network whose degree is given by the random variable  $D_T$  is

$$G_{X_T}(s) = G_{D_T}(G_I(s)), \quad (34)$$

where  $G_{D_T}(s) = \frac{1}{2} \left( G_{D_1^{(1)}}(s)G_{D_2^{(1)}}(s) \right) + \frac{1}{2} \left( G_{D_1^{(2)}}(s)G_{D_2^{(2)}}(s) \right)$  and  $G_I(s) = 1 - \rho + \rho s$ . Once we are beyond the seed node, we need to consider the excess offspring distribution,  $G_{\tilde{X}_T}(s) = G'_{X_T}(s)/G'_{X_T}(0)$  as we did in Sec. IV. This allows us to write down the relationship for the number of active nodes in the network without communities,  $\mathcal{N}_s(t)$ , from one generation to another as

$$\begin{aligned} G_{\mathcal{N}_s(t)}(s) &= G_{\mathcal{N}_s(t-1)}(G_{\tilde{X}_T}(s)) \text{ for } t > 1, \text{ and} \\ G_{\mathcal{N}_s(1)}(s) &= G_{\mathcal{N}_s(0)}(G_{X_T}(s)) \text{ for } t = 1, \end{aligned} \quad (35)$$

where  $G_{\mathcal{N}_s(0)}(s) = s$ . The PGF  $G_{\mathcal{N}_s(1)}(s)$  provides us with a way of constructing a *Simple Branching Process (SBP)* that has the same overall degree distribution as our multi-type branching process but without community structure. From this model, we can derive cascade size distributions and plot them in Fig. 6 alongside the cascades on the corresponding network with communities. From Fig. 6, we see that the simple branching

process model for a network without communities predicts a very different cascades size distribution than the model with communities. Thus the information diffusion on the community-based networks cannot be captured accurately with the Simple Branching Process. One notable effect takes place when we seed a cascade in community 1 and we have a large enough probability of infection,  $\rho = 0.12$ , the chance of observing larger cascades changes and displays quantitatively similar behaviour to those cascades seeded in community 2. We can speculate that this is due to activation probability being large enough that, if we observe a cascade of a certain size, it is likely to have spread to community 2, where the process takes advantage of the larger average degree within that community.

We can easily isolate the effect of communities by removing the inter-community links, setting  $p_e = 0$  to verify our interpretations. This allows the activations to spread within either community 1 or 2 only; see Fig. 7. We can note from Fig. 7 that it is indeed due to the community structure that community 1 sees a change in its cascade size distribution; however, if we seed activations in community 2, we see no such discernible benefit for community 2 being a connection to community 1, i.e., there is little change in its cascade size distribution when it is connected to the other community.

In this section, we have shown that our multi-type branching process model for information spread between communities can accurately model the spread of information between communities with a general network structure. This captures not only the effect of the community structure, where we have different internal connection structures within the communities, but also the effect of seeding infection in one community over the other. In the following section we provide some conclusions of our work and future directions.

## V. CONCLUSION

In this paper, we studied the information spreading process on a broad class of networks with community structures. We showed how, by using limited information about the network, specifically the degree distribution within and between the communities, we can calculate standard statistical characteristics of cascade dynamics. For this purpose, we developed a probability generating function theory to study how information spreads between and within communities. The methods developed in this study add to the theoretical tools for studying information diffusion on community-based networks or multiple connected networks.

Our framework allowed us to calculate important quantities of information diffusion, such as extinction probability, hazard function, and cascade size distribution, proving to be a simple and effective tool. Not only

did this tool enable us to accurately estimate the properties of dynamics on the entire network, but it also allowed us to extend these quantities to community-specific versions of characteristics of interest. This allowed us, for instance, to isolate the probability of extinction in a specific community. Additionally, we derive new quantities, specific to the information spread on a network with communities, such as the introduction and reintroduction probabilities. The introduction probability estimates (with high accuracy) the probability that the infection spreads to a new community, while the reintroduction represents the probability that a contagion, having ceased spreading in a specific community, might be reintroduced to that community at a later stage.

Finally, we analysed how information spreads across and within communities in a particular case in more details. We focused on a network that can be used to represent social networks, which was a graph with heavy-tailed (log-normal) distributed degree and sparsely distributed inter-community edges. We demonstrated how the initial seeding location of an infection affects the observed cascade size distribution. Furthermore, we compared the cascade dynamics on a network with communities to the dynamics on a network with the same degree distribution but no communities present. We showed that the presence of communities notably change the cascade dynamics on a heavy-tailed network and that our framework accurately captures the changes.

While this paper only discusses networks with two communities, our framework can be easily extended to accommodate any number of communities. This does not pose any theoretical challenges; the only complication will be the rapid increase in the number of random variables that need to be tracked as the number of communities increases. There are also several other directions that could be explored in future work. One natural extension would be incorporating a clique structure into the network within our framework. In the present paper, we require the network to have a local tree-like structure. The methods developed in [22, 23] will be a good starting point for this. Additionally, in the continuation of developing theoretical tools, it seems feasible to extend our methods to directed networks and networks with degree-degree correlations.

To further investigate the effect of communities on information spread, it may be interesting to study cases involving communities of varying sizes and determine whether the size of a community influences cascade dynamics, as it reasonably would. Another intriguing scenario involves introducing different types of nodes with varying probabilities of infection. This addition will not significantly complicate our analysis but will increase the number of random variables we need to track within our framework.

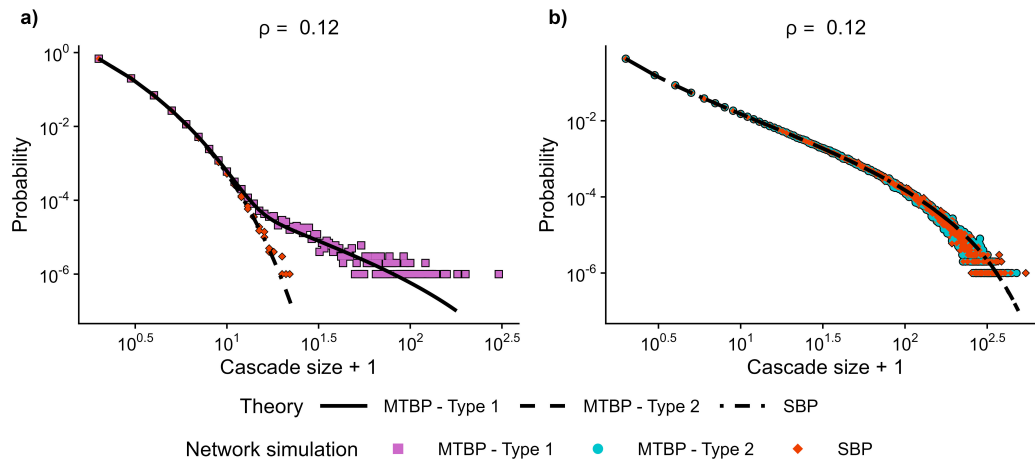


Figure 7: Cascade size distribution where  $\rho$  is fixed to 0.12. Solid and dashed lines represent  $p_e = 0.02$ , where cross-community spread is possible, and dot-dashed lines represent  $p_e = 0$ , where spread is confined to one community. a) Information spread behaviour when seeding in community 1 (which has an average degree of  $\approx 3$ ). b) Information spread behaviour when seeding in community 2 (which has an average degree of  $\approx 7$ ). As before, each community has 5000 nodes, totalling 10,000 nodes in the network. The internal connections in community 1 and community 2 use those stated in Fig. 5. Points represent the results of  $N_{sim} = 10^6$  Monte Carlo simulations of the ICM model on the network.

To enhance the applicability of our method described here, a comparison to real world data is a natural extension. Previous work [34] tracked information diffusion between and within communities for two conversation networks on Twitter (now X). The authors showed that users tend to communicate more frequently to other users in the same community than to users in the opposite community. But to what extent this is explained by the network structure and diffusion processes is an interesting and open question. The methodology introduced in this paper opens the door to the application to empirically observed cascades, to determine to what extent the network structure can explain the observed information diffusion process.

## FUNDING

This publication has emanated from research conducted with the financial support of Science Foundation Ireland under Grant numbers 18/CRT/6049 and 16/IA/4470, and European Research Council under the European Union’s Horizon 2020 research and innovation programme grant number 802421. For the purpose of Open Access, the authors have applied a CC BY public copyright licence to any Author Accepted Manuscript version arising from this submission.

## Appendix A: Numerical estimation of probabilities from probability generating functions

Let us first consider the case of the univariate probability-generating function

$$G_{N(t)}(s) = \sum_0^{\infty} P[N(t) = n] s^n. \quad (\text{A1})$$

By definition, the probability  $P[N(t) = n]$  is recovered from the PGF  $G_{N(t)}(s)$  as

$$P[N(t)] = \frac{1}{n!} \left[ \frac{d^n}{ds^n} (G_{N(t)}(s)) \right]_{(s=0)}. \quad (\text{A2})$$

By Cauchy’s theorem, we can transform this into a contour integral in the complex plane [31, 35] as

$$P[N(t) = n] = \frac{1}{2\pi i} \oint_C \frac{G_{N(t)}(s)}{s^{(n+1)}} ds, \quad (\text{A3})$$

where we can choose the unit circle for the contour  $C$  [35]. Next, replacing  $s = e^{i\omega}$ , we obtain

$$P[N(t) = n] = \frac{1}{2\pi} \int_0^{2\pi} G_{N(t)}(e^{i\omega}) e^{-in\omega} d\omega. \quad (\text{A4})$$

To calculate Eqn. (A4) numerically, we use the trapezoidal rule and divide the unit circle into  $K$  points. This yields

$$P[N(t) = n] \approx \frac{1}{K} \sum_{k=0}^{K-1} G_{N(t)}(e^{2\pi ik/K}) e^{2\pi ink/K}. \quad (\text{A5})$$

In turn, equation (A5) can be evaluated using standard fast Fourier transform numerical techniques [31, 36].

In the case of the bivariate PGF, the joint probability  $P[N_1(t) = n, N_2(t) = m]$  can be recovered from the bivariate PGF,  $G_{N(t)}(s_1, s_2)$ , as

$$P[N_1(t) = n, N_2(t) = m] = \frac{1}{n!m!} \left[ \frac{\partial^n}{\partial s_1^n} \frac{\partial^m}{\partial s_2^m} (G_{N(t)}(s_1, s_2)) \right]_{(s_1=0, s_2=0)}. \quad (\text{A6})$$

Similarly to the univariate case, if we substitute  $s_1 = e^{i\omega}$  and  $s_2 = e^{i\theta}$  into the expression for  $G_{N(t)}(s_1, s_2)$ ,

we can use 2-dimensional discrete Fourier transform to evaluate probabilities for the first  $K$  values for  $N_1(t)$  and  $N_2(t)$ . This yields

$$P[N_1(t) = n, N_2(t) = m] \approx \frac{1}{K^2} \sum_{k_1=0}^{K-1} \sum_{k_2=0}^{K-1} G_{N(t)}(e^{2\pi ik_1/K}, e^{2\pi ik_2/K}) e^{2\pi ink_1/K} e^{2\pi imk_2/K}. \quad (\text{A7})$$

## Appendix B: Recovering probabilities from probability generating functions

In this section we give detailed explanation on how the probabilities are recovered from the corresponding probability generating functions. As was explained in Sec. III, the probability generating function,  $G_{N(t)}$ , by definition is

$$G_{N(t)}(s_1, s_2) = \sum_{n=0}^{\infty} \sum_{m=0}^{\infty} P[N_1(t) = n, N_2(t) = m] s_1^n s_2^m. \quad (\text{B1})$$

As explained in Appendix A, the joint probability  $P[N_1(t) = n, N_2(t) = m]$  is given by the derivative of  $G_{N(t)}$ , as defined by (A6), and is evaluated using the discrete Fourier transform given by Eqn. (A7).

Now, let us discuss how we recover the probability of the number of active nodes in community 1 only. If we substitute  $s_2 = 1$  into Eqn.(B1) we obtain

$$G_{N(t)}(s_1, 1) = \sum_{n=0}^{\infty} P[N_1(t) = n] s_1^n. \quad (\text{B2})$$

and the probability  $P[N_1(t) = n]$  is straightforwardly recovered by

$$P[N_1(t) = n] = \frac{1}{n!} \left[ \frac{d^n}{ds_1^n} (G_{N(t)}(s_1, 1)) \right]_{s_1=0}. \quad (\text{B3})$$

To calculate this probability numerically, we apply discrete Fourier transform to function  $G_{N(t)}(s_1, 1)$  as fol-

lows

$$P[N_1(t) = n] \approx \frac{1}{K} \sum_{k=0}^{K-1} G_{N(t)}(e^{2\pi ik/K}, 1) e^{2\pi ink/K}. \quad (\text{B4})$$

Similarly, we apply discrete Fourier transform to  $G_{N(t)}(1, s_2)$  to evaluate the probability of the number of active nodes in community 2,  $P[N_2(t) = n]$ .

Finally, let us discuss how to obtain the probability of the total number of active nodes in the entire network,  $P[N_1(t) + N_2(t) = n]$ . To do this, we substitute  $s_1 = s$  and  $s_2 = s$  into  $G_{N(t)}$  to obtain

$$G_{N(t)}(s, s) = \sum_{n=0}^{\infty} \sum_{m=0}^{\infty} P[N_1(t) = n, N_2(t) = m] s^{n+m}. \quad (\text{B5})$$

Then the probability,  $P[N_1(t) + N_2(t) = n]$ , is calculated as follows

$$P[N_1(t) + N_2(t) = k] = \frac{1}{k!} \left[ \frac{d^k}{ds^k} (G_{N(t)}(s, s)) \right]_{s=0}. \quad (\text{B6})$$

which, in its turn, is evaluated with the discrete Fourier transform of  $G_{N(t)}(s, s)$  as follows

$$P[N_1(t) + N_2(t) = n] \quad (\text{B7})$$

$$\approx \frac{1}{K} \sum_{k=0}^{K-1} G_{N(t)}(e^{2\pi ik/K}, e^{2\pi ik/K}) e^{2\pi ink/K}. \quad (\text{B8})$$

### Appendix C: Comparing branching process simulations to network simulations

We compare our model using multi-type branching processes to network-based simulations and to the expected information diffusion using the mean-matrix to check the accuracy of the model. The mean-matrix  $M$  tracks the expected offspring of each type, so  $M_{ij}$  is the expected number of offspring from a node  $i$  that are of type  $j$  in the next time step. For the SBM we have the mean-matrix

$$M = \begin{pmatrix} \rho\lambda_{in} & \rho\lambda_{out} \\ \rho\lambda_{out} & \rho\lambda_{in} \end{pmatrix}.$$

If we start from a single seed in community 1, we can track the expected number of nodes by generation  $t$  in community 1 as

$$E[N_1(t)] = (1 \ 0) M^t \begin{pmatrix} 1 \\ 0 \end{pmatrix},$$

where  $t$  denote the matrix power and generation  $t$ . Similarly, if we are interested in tracking the number of active nodes in community 2 by generation  $t$  from a single seed in community 1 then we have

$$E[N_2(t)] = (1 \ 0) M^t \begin{pmatrix} 0 \\ 1 \end{pmatrix}.$$

We can then use this to compare our network-based simulations to the theory with the mean-matrix and to the branching processes simulations. We will see that all three have strong agreement in the subcritical case and for sufficiently large networks. Therefore, in some places, we will use branching processes simulations thanks to their ease of simulation.

Figure 8 shows the results obtained for 10,000 simulations for a range of values of infection probability  $\rho$  ( $\rho = 0.04$ ,  $\rho = 0.06$ ,  $\rho = 0.08$ ), expected number of edges inside a community  $\lambda_{in}$  ( $\lambda_{in} = 4$ ,  $\lambda_{in} = 8$ ) and expected number of edges between communities  $\lambda_{out}$  ( $\lambda_{out} = 0$ ,  $\lambda_{out} = 2$ ,  $\lambda_{out} = 4$ ) on a Poisson-distributed network. We use Stochastic Block Model networks containing 10,000 nodes split evenly between community 1 and community 2 and compare those to the equivalent multi-type branching process model for Poisson distribution. The simulations were set to start with the activation of one random node in community 1. There is cross-community information spread when  $\lambda_{out} > 0$ , in which case community 2 is expected to be infected on the first passage, on average. Fig. 8c) shows the offspring distribution for  $\rho = 0.08$ ,  $\lambda_{in} = 8$  and  $\lambda_{out} = 2$ . This is the combination of parameters among the considered values that generates the longest process. The process dies off earlier for the simulations

using  $\rho = 0.06$  (Fig. 8b)) and  $\rho = 0.04$  (Fig. 8a)) since the information survives shortly when the probability of infection is lower. When we consider no possibility of cross-community information spread ( $\lambda_{out} = 0$ , Fig. 8f)), we observe diffusion only inside community 1, and the overall process dies off earlier than the analogous with  $\lambda_{out} = 2$  (Fig. 8b)). On the other hand, when we increase  $\lambda_{out}$  (Fig. 8d)) information spreads further in both community 1 and community 2 in comparison to the analogous with lower  $\lambda_{out}$  values (Fig. 8b) and f)). When we keep  $\lambda_{out}$  moderate ( $\lambda_{out} = 4$ ) and decrease  $\lambda_{in}$  ( $\lambda_{in} = \lambda_{out} = 4$ ), with moderate probability of infection, the information dies out early.

Both the multi-type branching process and network-based simulations show good agreement with the theoretical expected results, suggesting that our model is accurate for large networks.

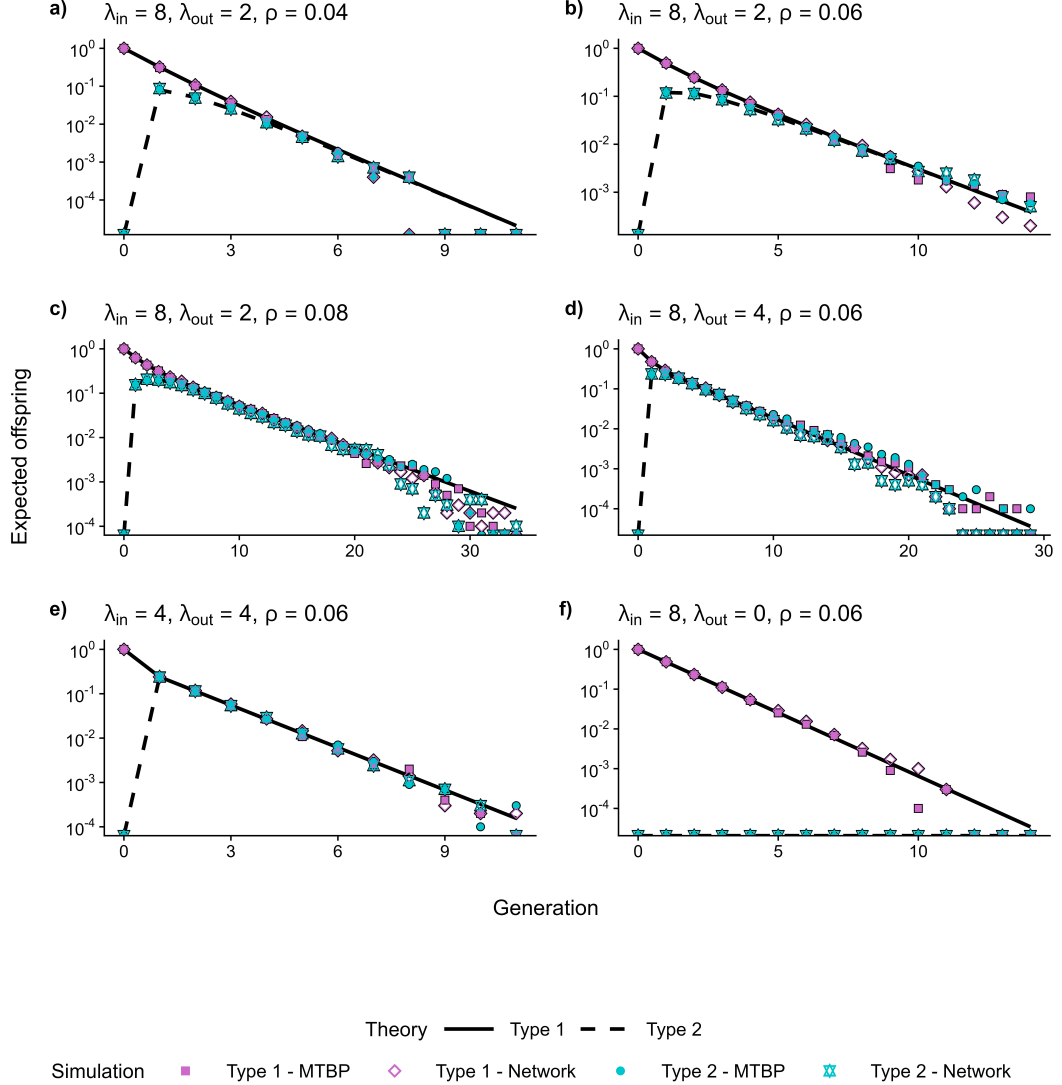


Figure 8: Distribution of expected offspring for various parameters. The shapes account for the multi-type branching process (MTBP) simulations and the network simulations, and the lines refer to the results given by the mean-matrix. a)  $\lambda_{\text{in}} = 8, \lambda_{\text{out}} = 2, \rho = 0.04$ : information spreads shortly overall; b)  $\lambda_{\text{in}} = 8, \lambda_{\text{out}} = 2, \rho = 0.06$ : moderate information spread overall; c)  $\lambda_{\text{in}} = 8, \lambda_{\text{out}} = 2, \rho = 0.08$ : long diffusion process overall; d)  $\lambda_{\text{in}} = 8, \lambda_{\text{out}} = 4, \rho = 0.06$ : information spreads further than in (b) but dies out slightly earlier than in (c), with moderate diffusion overall; e)  $\lambda_{\text{in}} = \lambda_{\text{out}} = 4, \rho = 0.06$ : information dies out early, comparable to (a); f)  $\lambda_{\text{in}} = 8, \lambda_{\text{out}} = 0, \rho = 0.06$ : information spreads only in community 1, with moderate diffusion.

#### Appendix D: Log-normal network parameter sweep

In this section we provide a parameter sweep for both  $\rho$  and  $p_e$ , and analyse the resultant distributions of cascade sizes. The network is the same as that presented in Sec. IV, namely where we have two communities of 5000 nodes, each with a log-normal distribution internally. Community 1 has  $\mu_1 = 0.85$  and  $\sigma_1 = 0.4$ , resulting in an internal average degree of 3. Community 2 has  $\mu_2 = 1.8$  and  $\sigma_2 = 0.4$ , resulting in an internal aver-

age degree of 7. The cross-community links are selected by adding single edges between nodes. We randomly select one node from community 1 and one node from community 2 and link them. The proportion of nodes selected is  $p_e$ .

Figure 9 shows the comparison of the theory and simulation under different values of  $p_e$ , where  $\rho$  is fixed. We can see that we have excellent agreement between our theory and simulations. As we increase the number of cross-community edges we have a general increase in

cascade size. This is most pronounced for those cascades seeded in community 1 (solid line).

Figure 10 provides the behaviour of our cross-community branching processes for various  $\rho$  values, where  $p_e$  is fixed to 1000/5000. We can note that we have excellent agreement between our theory and simulations in general. For larger  $\rho$  (most pronounced for  $\rho = 0.14$ ) values, we can note discrepancies between the theory and simulated values. The larger simulated cascade do not reach the same sizes as the theoretical cascades sizes. This is due to the finite size of the network, as for this value, cascades activate a significant proportion of the networks, while in the theory it is assumed that the networks are infinitely large.

### Appendix E: Constructing a multi-type branching process for $k$ -regular networks

In Sec. IV, we derived the required equations that describe the spread dynamics under the ICM through a network with two communities. Later, in Sec. IV A, we provided an example of how this works for a log-normally distributed network. As an aid to the reader, we provide here a simplified network example. We will assume the internal structure of the communities will be  $k$ -regular. Each node in community 1 will have in-community degree of 3 and each node in community 2 will have in-community degree of 7. As before, the probability of a node becoming active from an exposure in the previous timestep is  $\rho$ . This allows us to write down our PGF for the internal degree of each node in both communities, and their offspring distributions

$$\begin{aligned} G_{D_1^{(1)}}(s) &= s^3 \\ \Rightarrow G_{X_1^{(1)}}(s) &= G_{D_1^{(1)}}(G_I(s)) \\ &= (1 - \rho + \rho s)^3 \text{ and} \\ G_{D_2^{(2)}}(s) &= s^7 \\ \Rightarrow G_{X_2^{(2)}}(s) &= G_{D_2^{(2)}}(G_I(s)) \\ &= (1 - \rho + \rho s)^7, \end{aligned}$$

from which we can derive the required excess distributions using Eq. (29) as

$$\begin{aligned} G_{\tilde{X}_1^{(1)}}(s) &= G_{\tilde{D}_1^{(1)}}(G_I(s)) = (1 - \rho + \rho s)^2 \text{ and} \\ G_{\tilde{X}_2^{(2)}}(s) &= G_{\tilde{D}_2^{(2)}}(G_I(s)) = (1 - \rho + \rho s)^6. \end{aligned}$$

We assume, as we did in Sec. IV A, that each node has probability  $p_e$  of having 1 link between the communities,

$$\begin{aligned} G_{X_2^{(1)}}(s) &= G_{X_1^{(2)}}(s) \\ &= 1 - p_e + p_e(G_I(s)) \\ &= 1 - p_e + p_e(1 - \rho + \rho s), \end{aligned}$$

from which we can easily show that the excess offspring distributions for between-community spread are given by  $G_{\tilde{X}_2^{(1)}}(s) = G_{\tilde{X}_1^{(2)}}(s) = 1$ . Now we can proceed to create the offspring distribution for each of the 4 types that we have to track in our branching process. First, let us consider the PGF for the offspring from a node in community 1, who was activated from within its community. As it was activated from inside community 1, it will have one less neighbour that it can activate and this requires the use of the excess distribution, which is associated random variable  $\tilde{X}_1^{(1)}$ , while no



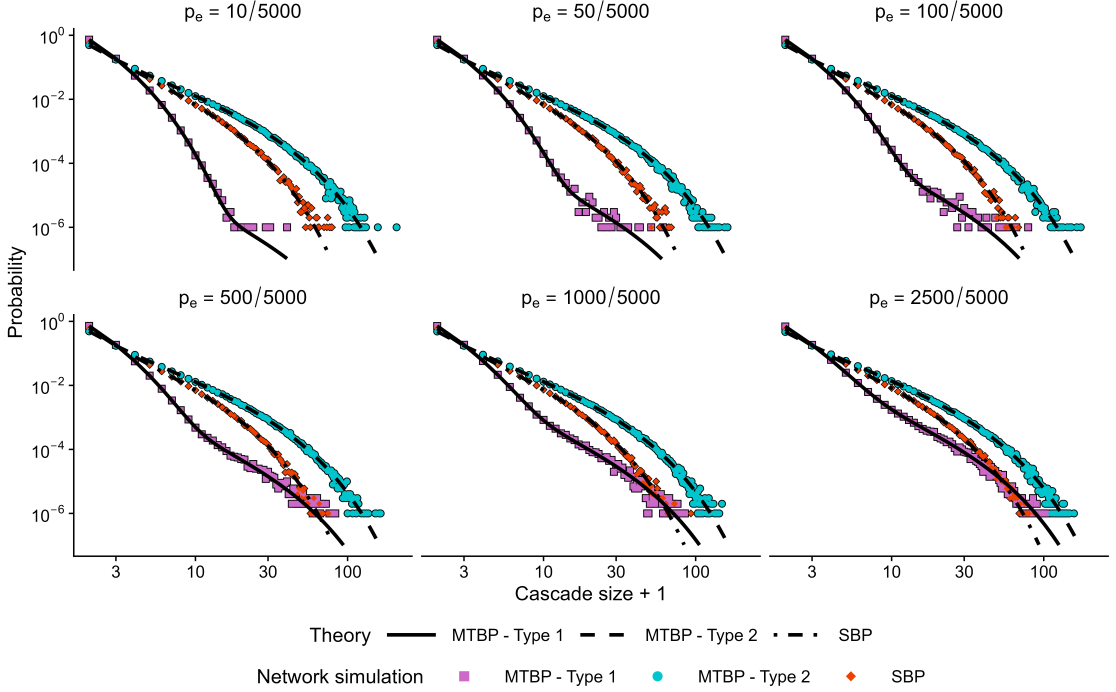


Figure 9: Parameter sweep, where  $\rho$  is fixed at 0.1 and  $p_e$  is swept from 10/5000 to 2500/5000. Each community has 5000 nodes, totalling 10000 nodes in the network. Lines represent theory curves, and the points represent the results of  $N_{sim} = 10^6$  Monte Carlo simulations of the ICM model on the network. Note that the middle dot-dashed line is for the corresponding simple branching process (which does not take into account community structure).

cross-community links we used in the activation, and so will use the cross-community degree distribution, which is associated with the random variable  $X_2^{(1)}$ , yielding the following offspring distribution:

$$G_{\mathbf{X}_{in}^{(1)}}(s_1^{in}, s_2^{out}) = G_{\tilde{X}_1^{(1)}}(s_1^{in})G_{X_2^{(1)}}(s_2^{out}) \\ = (1 - \rho + \rho s_1^{in})^2 (1 - p_e + p_e(1 - \rho + \rho s_2^{out})).$$

When deriving  $G_{\mathbf{X}_{out}^{(1)}}$  the same logic holds, but as the node was activated by from outside of community 1, therefore, it will still have its full complement of in-community nodes that it can activate, requiring the use of  $X_1^{(1)}$  and the use of the excess between-community offspring distribution, with associated random variable  $\tilde{X}_2^{(1)}$ . The yielding the following offspring distribution

$$G_{\mathbf{X}_{out}^{(1)}}(s_1^{in}, s_2^{out}) = G_{X_1^{(1)}}(s_1^{in})G_{\tilde{X}_2^{(1)}}(s_2^{out}) \\ = (1 - \rho + \rho s_1^{in})^3 (1).$$

And we can easily extend this to find the offspring distributions for community 2, which will be

$$G_{\mathbf{X}_{in}^{(2)}}(s_2^{in}, s_1^{out}) = G_{\tilde{X}_2^{(2)}}(s_2^{in})G_{X_1^{(2)}}(s_1^{out}) \\ = (1 - \rho + \rho s_2^{in})^6 (1 - p_e + p_e(1 - \rho + \rho s_1^{out})) \text{ and} \\ G_{\mathbf{X}_{out}^{(2)}}(s_2^{in}, s_1^{out}) = G_{X_2^{(2)}}(s_2^{in})G_{\tilde{X}_1^{(2)}}(s_1^{out}) \\ = (1 - \rho + \rho s_2^{in})^6 (1).$$

To find the number of nodes active at time  $t$  we just need to consider what happens between generation 0 and 1. If we seed the process with one active individual in community 1 at time  $t = 0$ , then our initial conditions are  $G_{\mathcal{N}(1)}(s) = (s)^1$ . Then as the process has just started the active node has no previously active neighbours, therefore, the offspring distribution is given by

$$G_{\mathcal{N}(1)}(s_1^{in}, s_1^{out}, s_2^{in}, s_2^{out}) = G_{\mathbf{X}^{(1)}}(s_1^{in}, s_1^{out}, s_2^{in}, s_2^{out}) \\ = G_{X_1^{(1)}}(s_1^{in})G_{X_2^{(1)}}(s_2^{out}) \\ = (1 - \rho + \rho s_1^{in})^3 (1 - p_e + p_e(1 - \rho + \rho s_2^{out})).$$

Now we can iterate this function to the desired number of generations, for example, to find the number of active nodes by generation 2, we can note that

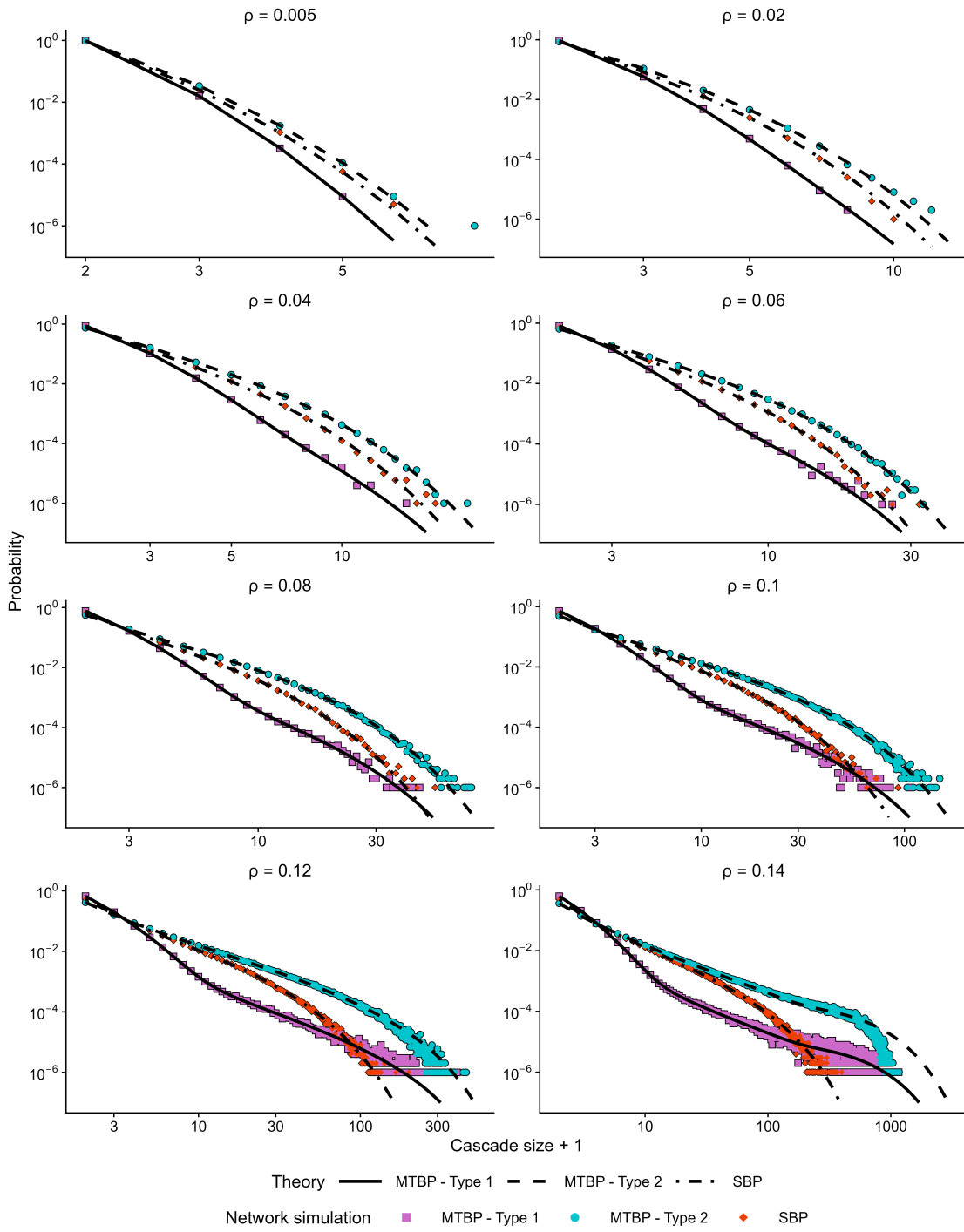


Figure 10: Parameter sweep, where  $p_e$  is fixed at 1000/5000 and  $\rho$  is swept from 0.005 to 0.14. Each community has 5000 nodes, totalling 10000 nodes in the network. Lines represent theory curves, and the points represent the results of  $N_{sim} = 10^6$  Monte Carlo simulations of the ICM model on the network. Note that the middle dot-dashed line is for the corresponding simple branching process (which does not take into account community structure).

$$\begin{aligned}
G_{\mathcal{N}(2)}(s_1^{in}, s_1^{out}, s_2^{in}, s_2^{out}) &= G_{\mathcal{N}(1)}(G_{\mathbf{X}_{in}^{(1)}}, G_{\mathbf{X}_{out}^{(1)}}, G_{\mathbf{X}_{in}^{(2)}}, G_{\mathbf{X}_{out}^{(2)}}) \\
&= (1 - \rho + \rho(G_{\mathbf{X}_{in}^{(1)}}))^3 \left(1 - p_e + p_e(1 - \rho + \rho(G_{\mathbf{X}_{out}^{(2)}}))\right) \\
&= (1 - \rho + \rho(1 - \rho + s_1^{in}\rho)^2(1 - p_e + (1 - \rho + s_2\rho)p_e))^3 \times \\
&\quad (1 - p_e + (1 - \rho + \rho(1 - \rho + s_2^{in}\rho)^7)p_e).
\end{aligned}$$

---

This process can be continued to find later generations, which, for small  $t$  can be found easily using symbolic solvers; however, for a later generations the use of symbolic solvers becomes computationally expensive requiring methods of inverting probability generations need to be used, which we have discussed in App. A4. We also make use of additional types when we wish to calculate a probability generating function for the total cascade size. Effectively, this new particle type is generated every time a node is active, but they themselves never die. This addition of counter types results in the ability of to count the number of active node created by time  $t$ . Let  $c$  be a dummy variable for this new type, in the last example our initial conditions would now be,

$$G_{\mathcal{C}(0)}(s, c) = (s)^1 c.$$

Then the  $t = 1$  generation would be

$$\begin{aligned}
G_{\mathcal{C}(1)}(s_1^{in}, s_1^{out}, s_2^{in}, s_2^{out}, c, c) &= G_{\mathbf{X}^{(1)}}(s_1^{in}c, s_2^{out}c, c) \\
&= G_{\mathbf{X}_1^{(1)}}(s_1^{in}c)G_{\mathbf{X}_2^{(1)}}(s_2^{out}c)c \\
&= (1 - \rho + \rho s_1^{in}c)^3 (1 - p_e + p_e(1 - \rho + \rho s_2^{out}c))c.
\end{aligned}$$

We iterate similarly to the previous example to arrive at the required PGF

$$\begin{aligned}
G_{\mathcal{C}(2)}(s_1^{in}, s_1^{out}, s_2^{in}, s_2^{out}, c, c) \\
&= (1 - \rho + c\rho(1 - \rho + cs_1^{in}\rho))^2 \times \\
&\quad (1 - p_e + (1 - \rho + cs_2^{out}\rho)p_e))^3 \times \\
&\quad (1 - p_e + (1 - \rho + c\rho(1 - \rho + cs_2^{in}\rho)^7)p_e)c,
\end{aligned}$$

and this process is repeated until the required generation has been reached. We can then marginalised the required types in the PGF to recover the univariate PGF for the cascade size distribution, for example, by  $G_{\mathcal{C}(t)}(1, 1, 1, 1, c)$ . Then this can be inverted via inverse fast Fourier transform to obtain the probability mass function, see App. A4. It should be noted that this entire process is no more complex for general degree distributions once we have the network structure, just a little more cumbersome.

- 
- [1] Jacob Amedie. The Impact of Social Media on Society. Pop Culture Intersections, September 2015.
- [2] Shannon E. Clark, Megan C. Bledsoe, and Christopher J. Harrison. The role of social media in promoting vaccine hesitancy. Current Opinion in Pediatrics, 34(2):156–162, April 2022.
- [3] Neil F. Johnson, Nicolas Velásquez, Nicholas Johnson Restrepo, Rhys Leahy, Nicholas Gabriel, Sara El Oud, Minzhang Zheng, Pedro Manrique, Stefan Wuchty, and Yonatan Lupu. The online competition between pro-and anti-vaccination views. Nature, 582(7811):230–233, June 2020. Number: 7811 Publisher: Nature Publishing Group.
- [4] Israel Junior Borges Do Nascimento, Ana Beatriz Pizarro, Jussara M Almeida, Natasha Azzopardi-Muscat, Marcos André Gonçalves, Maria Björklund, and David Novillo-Ortiz. Infodemics and health misinformation: a systematic review of reviews, 2022.
- [5] Mariano Beguerisse-Díaz, Amy K. McLennan, Guillermo Garduño-Hernández, Mauricio Barahona, and Stanley J. Ulijaszek. The ‘who’ and ‘what’ of #diabetes on Twitter. Digital Health, 3:2055207616688841, January 2017. Publisher: SAGE Publications Ltd.
- [6] Edited by Joshua A. Tucker and Nathaniel Persily. Social Media and Democracy: The State of the Field, Prospects for Reform. August 2020. ISBN: 9781108890960 Publisher: Cambridge University Press.
- [7] Sinan Aral, Lev Muchnik, and Arun Sundararajan. Distinguishing influence-based contagion from homophily-driven diffusion in dynamic networks. Proceedings of the National Academy of Sciences, 106(51):21544–21549, December 2009.
- [8] Marián Boguná, Romualdo Pastor-Satorras, and Alessandro Vespignani. Absence of epidemic threshold in scale-free networks with degree correlations. Physical review letters, 90(2):028701, 2003.
- [9] Joel C. Miller. Percolation and epidemics in random clustered networks. Physical Review E, 80(2):020901, August 2009. Publisher: American Physical Society.
- [10] Mason Porter and James Gleeson. Dynamical Systems on Networks: A Tutorial, volume 4 of Frontiers in Applied Dynamical Systems: Reviews and Tutorials. Springer International Publishing, Cham, 2016.
- [11] Lilian Weng, Filippo Menczer, and Yong-Yeol Ahn. Virality Prediction and Community Structure in Social Networks. Scientific Reports, 3(1):2522, August 2013.
- [12] Fan Zhou, Xovee Xu, Goce Trajcevski, and Kunpeng Zhang. A Survey of Information Cascade Analysis: Models, Predictions, and Recent Advances. ACM Computing Surveys, 54(2):1–36, March 2022.
- [13] Minh X. Hoang, Xuan-Hong Dang, Xiang Wu, Zhenyu Yan, and Ambuj K. Singh. GPPOP: Scalable Group-level Popularity Prediction for Online Content in Social Networks. In Proceedings of the 26th International Conference on World Wide Web, pages 725–733, Perth Australia, April 2017. International World Wide Web Conferences Steering Committee.
- [14] Lilian Weng, Filippo Menczer, and Yong-Yeol Ahn. Predicting Successful Memes Using Network and Community Structure. Proceedings of the International AAAI Conference on Web and Social Media, 8(1):535–544, May 2014.
- [15] Clara Stegehuis, Remco Van Der Hofstad, and Johan S. H. Van Leeuwen. Epidemic spreading on complex networks with community structures. Scientific Reports, 6(1):29748, July 2016.
- [16] Jinxian Li, Jing Wang, and Zhen Jin. SIR dynamics in random networks with communities. Journal of Mathematical Biology, 77(4):1117–1151, October 2018.
- [17] Yuchen Li, Ju Fan, Yanhao Wang, and Kian-Lee Tan. Influence Maximization on Social Graphs: A Survey. IEEE Transactions on Knowledge and Data Engineering, 30(10):1852–1872, October 2018.
- [18] Manuel Gomez-Rodriguez, Jure Leskovec, and Andreas Krause. Inferring Networks of Diffusion and Influence. ACM Transactions on Knowledge Discovery from Data, 5(4):1–37, February 2012.
- [19] Tiago P. Peixoto. Network Reconstruction and Community Detection from Dynamics. Physical Review Letters, 123(12):128301, September 2019.
- [20] Charles D. Brummitt, Raissa M. D’Souza, and E. A. Leicht. Suppressing cascades of load in interdependent networks. Proceedings of the National Academy of Sciences, 109(12), March 2012.
- [21] James P Gleeson, Tomokatsu Onaga, Peter Fennell, James Cotter, Raymond Burke, and David J P O’Sullivan. Branching process descriptions of information cascades on Twitter. Journal of Complex Networks, 8(6):cnab002, March 2021.
- [22] Leah A. Keating, James P. Gleeson, and David J. P. O’Sullivan. Multitype branching process method for modeling complex contagion on clustered networks. Physical Review E, 105(3):034306, March 2022. Publisher: American Physical Society.
- [23] Leah A Keating, James P Gleeson, and David J P O’Sullivan. A generating-function approach to modelling complex contagion on clustered networks with multi-type branching processes. Journal of Complex Networks, 11(6):cnad042, November 2023.
- [24] David Kempe, Jon Kleinberg, and Éva Tardos. Maximizing the spread of influence through a social network. In Proceedings of the ninth ACM SIGKDD international conference on Knowledge discovery and data mining, KDD ’03, pages 137–146, New York, NY, USA, August 2003. Association for Computing Machinery.
- [25] Kristina Lerman. Information Is Not a Virus, and Other Consequences of Human Cognitive Limits. Future Internet, 8(2):21, June 2016. Number: 2 Publisher: Multidisciplinary Digital Publishing Institute.
- [26] Hal Caswell. Matrix Population Models: Construction, Analysis, and Interpretation. Ecological Modelling, 148(3):307–310, March 2002.
- [27] Mark Newman. Networks, volume 1. Oxford University Press, October 2018.
- [28] Marek Kimmel and David E. Axelrod. Branching

- Processes in Biology, volume 19 of Interdisciplinary Applied Mathematics. Springer New York, New York, NY, 2002.
- [29] Paul W. Holland, Kathryn Blackmond Laskey, and Samuel Leinhardt. Stochastic blockmodels: First steps. Social Networks, 5(2):109–137, June 1983.
- [30] James P. Gleeson, Jonathan A. Ward, Kevin P. O’Sullivan, and William T. Lee. Competition-induced criticality in a model of meme popularity. Physical Review Letters, 112(4):048701, January 2014.
- [31] J. K. Cavers. On the fast fourier transform inversion of probability generating functions. IMA Journal of Applied Mathematics, 22(3):275–282, 1978.
- [32] Patsy Haccou, Peter Jagers, and Vladimir A Vatutin. Branching processes: variation, growth, and extinction of populations. Number 5. Cambridge university press, 2005.
- [33] Geoffrey Grimmett and David Stirzaker. Probability and random processes. Oxford university press, 2020.
- [34] Caroline Pena, Pádraig MacCarron, and David J. P. O’Sullivan. Finding polarised communities and tracking information diffusion on Twitter: The Irish Abortion Referendum. arXiv preprint arXiv:2311.09196, 2023.
- [35] Mark EJ Newman, Steven H Strogatz, and Duncan J Watts. Random graphs with arbitrary degree distributions and their applications. Physical review E, 64(2):026118, 2001.
- [36] M Marder. Dynamics of epidemics on random networks. Physical Review E, 75(6):066103, 2007.